

# A Production Routing Problem with Mobile Inventories

Raian Lefgoum\*    Sezin Afsar†    Pierre Carpentier‡  
 Jean-Philippe Chancelier\*    Michel De Lara\*

March 6, 2025

## Abstract

Hydrogen is an energy vector, and one possible way to reduce CO<sub>2</sub> emissions. This paper focuses on a hydrogen transport problem where mobile storage units are moved by trucks between sources to be refilled and destinations to meet demands, involving swap operations upon arrival. This contrasts with existing literature where inventories remain stationary. The objective is to optimize daily routing and refilling schedules of the mobile storages. We model the problem as a flow problem on a time-expanded graph, where each node of the graph is indexed by a time-interval and a location and then, we give an equivalent Mixed Integer Linear Programming (MILP) formulation of the problem. For small to medium-sized instances, this formulation can be efficiently solved using standard MILP solvers. However, for larger instances, the computational complexity increases significantly due to the highly combinatorial nature of the refilling process at the sources. To address this challenge, we propose a two-step heuristic that enhances

solution quality while providing good lower bounds. Computational experiments demonstrate the effectiveness of the proposed approach. When executed over the large-sized instances of the problem, the median (resp. the mean) obtained by this two-step heuristic outperforms the median (resp. the mean) obtained by the direct use of the MILP solver by 12.7% (resp. 9%), while also producing tighter lower bounds. These results validate the efficiency of the method for optimizing hydrogen transport systems with mobile storages and swap operations.

**Keywords** Production routing problem · Hydrogen mobile storage · Mixed-Integer Linear Program

## 1 Introduction

The global shift towards sustainable energy solutions has underscored the importance of hydrogen as a key component in reducing CO<sub>2</sub> emissions and addressing climate change concerns. Hydrogen not only offers a clean alternative fuel source, but also enhances energy security and flexibility. To support the expanding hydrogen economy, efficient transportation and distribution systems are essential for meeting (mobility) demands while minimizing operational costs.

\*Cermics, École Nationale des Ponts et Chaussées, IP Paris, 6 et 8 avenue Blaise Pascal, 77455 Marne la Vallée Cedex 2

†Universidad de Oviedo, Gijón, Principality of Asturias, Spain

‡UMA, ENSTA Paris, IP Paris, France

In this paper, we address an optimal transport problem in which trucks are used to transport mobile hydrogen storage units (tanks) between *sources* and *destinations*. The sources represent supply locations where the storages are refilled with hydrogen, while the destinations correspond to sites where the stored hydrogen is consumed to meet mobility demands. The transport process operates bidirectionally, as storages are transported from sources to destinations to satisfy the demand and storages are also transported back from destinations to sources for refilling, ensuring a continuous supply cycle. Within a specified planning horizon, the transport problem objective is to find daily routing and refilling schedules of mobile storage units, in order to minimize an intertemporal cost taking into account transport, hydrogen purchase and demand dissatisfaction costs.

This work focuses on a variant of the Production Routing Problem (PRP), where mobile storages are moved by trucks between sources and destinations. Unlike conventional routing problems that assume static inventories [5, 10] at delivery locations, we use the concept of mobile inventories, allowing for dynamic relocation and swap operations upon delivery which are specific to hydrogen transport. This added layer of complexity requires optimizing daily routing and refilling schedules for mobile storage units.

Another distinguishing feature of this work, compared to the PRP found in the literature, is the highly combinatorial nature of the refilling process at the sources. This complexity arises from three factors: the constraint that exactly one storage unit must be present at each destination at any given time to satisfy demand, the constraint on the refilling capacity at the sources, and the fact that the stock of mobile storage units at the

sources cannot be mixed. Specifically, when a new storage unit arrives from a source to replace the one previously stationed at the destination, the departing storage may not be empty, as it must be replaced immediately upon the arrival of the new mobile storage. As a result, multiple partially filled storage units may return to the same source, these units may also depart the next day without reaching full capacity because of refilling capacity at the sources. This, combined with the restriction on stock mixing, increases the complexity of the refilling process, as discussed later in §5.2.4.

Now, we describe some assumptions that we make on the movements of storage units. When a storage unit is transported by truck from a source location to a destination location, an operation we refer to as a *swap upon arrival* is to be performed at destination: the truck exchanges the storage unit it carries with a storage unit located at the destination. Then, the newly positioned storage unit serves to meet demand at destination, while the collected storage returns to a source for refilling, transported by the same truck. To simplify the problem, we assume that *the trip initialized by a truck on a specific day is completed within the same day*. Moreover, we assume that, at initial time, there is a single storage unit at each destination. Then, during the optimization time span, we always have *a single storage unit to meet demand at each destination* (see Fig. 1). Moreover, we assume that each destination can receive at most one storage per day, that is, there is at most one swap per destination and per day. Using the previous assumptions, the delivery planning of storage units is done on a daily basis. Firstly, we need to determine what happens to the storage units at the source locations: whether they stay where they are

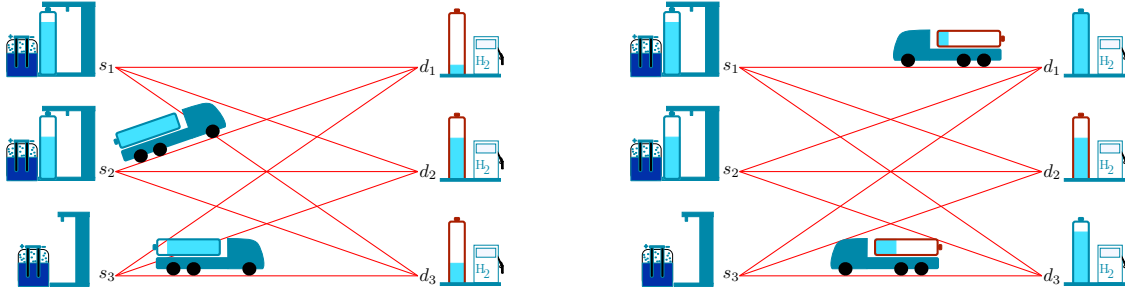


**Figure 1:** Storage unit delivery (left) and back to source after swap (right)

or they be delivered to a destination. Second, we decide which source location the collected storage unit goes to.

Daily refill planning of the storage units involves determining the quantity of hydrogen to be purchased per source location per day. The daily maximum quantity of hydrogen purchased is assumed to be bounded. Moreover, when several storage units are present at a given source, the allocation of the purchased hydrogen between the present storage units is to be decided.

The rest of the paper is organized as follows. We review the existing literature in this field in Sect. 2. Afterwards, in Sect. 3, we give the notations and assumptions for our problem. We introduce the problem on a time-expanded graph in Sect. 4, and give its model in Sect. 5. In Sect. 6, we give the problem formulation and describe in detail the different algorithms. Numerical experiments are presented in Sect. 7. In Sect. 8, we demonstrate how the storage routes (transport planning) can be derived from a solution of the problem on this time-expanded flow graph and finally the conclusion and possible directions for future works are discussed in Sect. 9.

## 2 Literature review

Logistics and transport optimization have long been critical areas of research, with the *Vehicle Routing Problem* (VRP) (see for example [7, 22, 23]) serving as a foundational framework for optimizing the delivery of goods and services. Extending the VRP, the *Inventory Routing Problem* (IRP) [11] integrates inventory management with routing decisions, while the *Production Routing Problem* (PRP) [2] further incorporates production planning.

As a generalization of the VRP, the IRP and PRP share its classification as an NP-hard problem [17] which means that there is no known algorithm that can solve the IRP and PRP efficiently (in polynomial time).

Moreover, aside from the classical IRP and PRP, a wide range of variants have been studied in the literature. As an example, the IRP with transshipment [10] and PRP with transshipment [6] enable the transfer of goods between delivery locations, offering greater flexibility but introducing additional decision variables, whereas the IRP with pickup and delivery [5] and PRP with pickup and delivery [9] allow vehicles to visit pickup locations during their routes. These pickups can either be used for future deliveries or stored at the depot after completing the route. In [8], the

authors propose a randomized local search algorithm to address large-scale instances of the IRP, that incorporates practical constraints such as time windows, driver safety, and site accessibility for vehicle resources. Additionally, they introduce a surrogate objective that ensures that short-term optimization solutions yield favorable long-term outcomes.

Several studies have examined real-life routing problems within the gas and hydrogen sectors [3, 15, 21, 24, 25]. In [3], a model for the liquefied natural gas sector is explored, introducing a decomposition algorithm using a path flow model with pre-generated duties and added valid inequalities. In [15], the Stochastic Cyclic Inventory Routing Problem is addressed with supply uncertainty, applied to green hydrogen distribution in the Northern Netherlands. The study proposes a combined approach using a parameterized Mixed Integer Programming model for static, periodic vehicle transportation schedules and a Markov Decision Process to optimize dynamic purchase decisions under stochastic supply and demand. In [21], the authors study a green PRP for medical nitrous oxide ( $N_2O$ ) supply chains, integrating cost minimization and GHG emission reduction. A bi-objective model with a Branch-and-Cut algorithm and Fuzzy Goal Programming is developed to optimize production, transportation, and environmental impact. In [24], the authors develop an optimization model for the integrated operation of an Electric Power and Hydrogen Energy System (IPHS), combining unit commitment, hydrogen production, transportation, and refueling. They formulate hydrogen transportation as a Vehicle Routing Problem (VRP) to optimize delivery routes. The overall problem is solved using an Augmented Lagrangian Decomposition method by dualizing the constraints

linking the hydrogen production and transportation models. In [25], a MILP model is developed for optimizing distribution and inventory in industrial gas supply chains, integrating vehicle routing with tank sizing to minimize costs. However, all these works typically assume fixed inventories.

In contrast, in this paper we focus on a novel variant of the PRP involving *mobile inventories*. This problem arises in the context of hydrogen distribution, where mobile storage units at destinations must be swapped and transported to other locations. To the best of our knowledge, studying this type of PRP, especially in the context of hydrogen transport, is new.

More precisely, the contributions of this paper are the following.

- We tackle a case study from an industrial partner about a hydrogen delivery problem.
- We introduce a new class of problems that we call *Production Routing Problem with Mobile Inventories* (PRP-MI). As already mentioned, PRP-MI are characterized by the fact that mobile storages at destinations can be swapped and transported to other locations. Additionally, since these mobile storages can arrive partially filled and depart without reaching full capacity, the refilling process at the sources presents a combinatorial challenge that must be taken into account in the model. In our study, these mobile storages are used for hydrogen distribution, however, the proposed framework can be applied to other transport problems with other commodities and similar logistical challenges.
- We propose a formulation of a PRP-MI optimization problem on a time-

expanded graph and present an equivalent Mixed Integer Linear Program (MILP) model.

- We propose a two-step heuristic approach to effectively solve large-scale instances of the PRP-MI. First, this heuristic simplifies the problem by omitting the combinatorial constraints of the refilling process at the sources to obtain a transport plan for the storages. Second, it optimizes the quantities purchased at the sources and their allocation to the storages.
- We conduct comprehensive numerical experiments to compare the performance of three different methods for solving the PRP-MI, evaluating their solution quality across diverse problem instances.

### 3 Problem notations and assumptions

In this section, we turn the problem narrative given in the introduction to a more formal optimization problem description, and give all assumptions of the problem.

For that purpose, we start by introducing some notations. We denote by  $\mathbb{J} = \{1, \dots, J\}$  the set of days of the optimization planning horizon. Moreover, to follow the problem narrative and as suggested in Fig. 1, we need to refer to the time-intervals before and after a swap at each destination. For that purpose we introduce two sets related to day specification, the set  $\underline{\mathbb{J}} = \{\underline{j} \mid j \in \mathbb{J}\}$  (resp. the set  $\overline{\mathbb{J}} = \{\overline{j} \mid j \in \mathbb{J}\}$ ), where for a day  $j$ , the notation  $\underline{j}$  stands for the first part of the day, when decisions to move storages from sources are made (resp.  $\overline{j}$  stands for the second part of the day, when deciding to which

source to return a storage unit after a swap at destination). We then consider the set  $\widehat{\mathbb{J}} = (\underline{\mathbb{J}} \cup \overline{\mathbb{J}}) \cup \{\overline{0}\}$  which is equipped with a finite total order:

$$\overline{0} \preceq \underline{1} \preceq \overline{1} \preceq \dots \preceq \underline{J} \preceq \overline{J}, \quad (1)$$

and where  $\overline{0}$  is an extra time index at which the initial conditions of the problem are given (see Figure 4). For  $i \in \widehat{\mathbb{J}}$ , we denote by  $i^+$  the successor (resp. by  $i^-$  the predecessor) of time  $i$  if it exists in the total order  $(\widehat{\mathbb{J}}, \preceq)$ :

$$\begin{aligned} \forall j \in \mathbb{J}, \quad (j)^+ &= \overline{j}, \quad (j)^- = \overline{j-1}, \\ \forall j \in \mathbb{J} \setminus \{J\}, \quad (\overline{j})^+ &= \underline{j+1}, \\ \forall j \in \mathbb{J}, \quad (\overline{j})^- &= \underline{j}. \end{aligned}$$

The hours within a day are denoted by  $\mathbb{H} = \{0, \dots, 23\}$  and we denote by  $\underline{h} = 0$  the smallest (resp.  $\overline{h} = 23$  the greatest) element of  $\mathbb{H}$ .

We also denote by  $\mathbb{S}$  the set of sources, by  $\mathbb{D}$  the set of destinations (also called stations), and by  $\mathbb{B}$  the set of mobile storage units. We denote by  $\mathcal{G} = (\mathcal{V}, \mathcal{E})$  the undirected transportation graph. The set of nodes  $\mathcal{V}$  is the disjoint union of the sources and destinations, that is  $\mathcal{V} = \mathbb{S} \sqcup \mathbb{D}$ . As we assume that there is no transport between two destinations or two sources, the graph  $\mathcal{G}$  is a bipartite graph with respect to  $\mathbb{S}$  and  $\mathbb{D}$ . Without loss of generality, the graph  $\mathcal{G}$  is assumed to be complete, meaning that each destination is reachable from any source and vice-versa with known transport times that are not necessarily symmetric. Specifically, the transport time from a source  $s$  to a destination  $d$ , denoted as  $t_{s,d}$ , may differ from the transport time from the same destination  $d$  back to the same source  $s$ , denoted as  $t_{d,s}$ . In addition to the transport time between a source and a destination, we consider a mapping  $g : \mathbb{S} \times \mathbb{D} \rightarrow \mathbb{R}_+$  which for a given oriented pair  $(s, d)$ ,  $g(s, d)$  gives the

sum of three terms: the time needed to load the truck with a storage unit at the source  $s$ ; the transport time from  $s$  to  $d$ ; the swap time of the storage units at the destination  $d$ .

For any set  $\mathbb{A}$ , we denote by  $\mathbf{1}_{\mathbb{A}}(\cdot)$  the indicator function of  $\mathbb{A}$  that equals 1 when its argument belongs to  $\mathbb{A}$  and 0 otherwise, by  $\Delta_{\mathbb{A}}$  the diagonal set  $\Delta_{\mathbb{A}} = \{(a, a) \mid a \in \mathbb{A}\} \subset A^2$  and, when  $\mathbb{A}$  is finite, by  $|\mathbb{A}|$  its cardinality. Finally, for all  $n \in \mathbb{N}$ , where  $\mathbb{N}$  is the set of natural numbers, we denote the set  $\{1, \dots, n\}$  by  $[n]$ .

The following assumptions are made on the transport model:

- $A_1$  : All mobile storage units have the same maximal capacity, denoted by  $\bar{S}$ ;
- $A_2$  : The maximal capacity  $\bar{S}$  is designed to meet at least one day's demand at any destination;
- $A_3$  : Each destination can receive at most one storage per day;
- $A_4$  : Each storage is transported at most once per day;
- $A_5$  : Each truck departing from a source  $s \in \mathbb{S}$  starts at a given predetermined hour in the morning  $h_0$ ;
- $A_6$  : The maximum number of storage units that can stay at source  $s \in \mathbb{S}$  is bounded by  $\kappa(s) \in \mathbb{N}$ ;
- $A_7$  : There is no refill at the sources during the first part of the day;
- $A_8$  : There is always exactly one storage per destination per day (except during a swap).

As introduced previously, we have two time scales in the transport problem, a day time scale ( $\mathbb{J}$ ) and an hour time scale ( $\mathbb{H}$ ). We

have introduced a day split in two parts in the previously and we give now the consequence of this day split at hour level. Given a source  $s$  from which a storage unit is sent to a destination  $d$ , the end of the swap at destination will occur at hour  $h_0 + g(s, d)$  using Assumption  $A_4$  and  $A_5$  and the definition of the mapping  $g$ . At each destination  $d \in \mathbb{D}$ , we divide each day  $j$  duration into two time periods: the first part of the day which is the time period  $[\underline{h}, h_{s,d,j}^{\text{sw}}[$  from midnight ( $\underline{h}$ ) to  $h_{s,d,j}^{\text{sw}}$ , where  $h_{s,d,j}^{\text{sw}}$  denotes the hour at which the swap ends at destination  $d$  at day  $j$  and the last, or second, part of the day which is the time period  $[h_{s,d,j}^{\text{sw}}, \bar{h} + 1[$  from the end of swap until midnight ( $\bar{h} + 1$ ). Indeed, using the definition of the function  $g$  and of time  $h_0$ , we have that  $h_{s,d,j}^{\text{sw}} = h_0 + g(s, d)$ , where  $s$  is the source from which the storage unit was transported to  $d$  on day  $j$ . Together with Assumption  $A_3$ , during a fixed day, we obtain that at most two distinct storages are used to fulfill the demand, one for each time period. Finally, if during day  $j$  no storage is sent to destination  $d$ , there is no swap time at destination and we arbitrarily divide the day into two time periods, which will be explained in more details later in Equation (14). An example of a swap is illustrated in Fig. 2.

## 4 Problem description on a time-expanded flow graph

In the context of routing problems with a fleet of vehicles, previous studies (e.g., [1, 4]) have demonstrated that vehicle-indexed formulations yield high-quality solutions when considering complete tours and a limited number of vehicles (typically fewer than five). However, our problem differs in that the routes

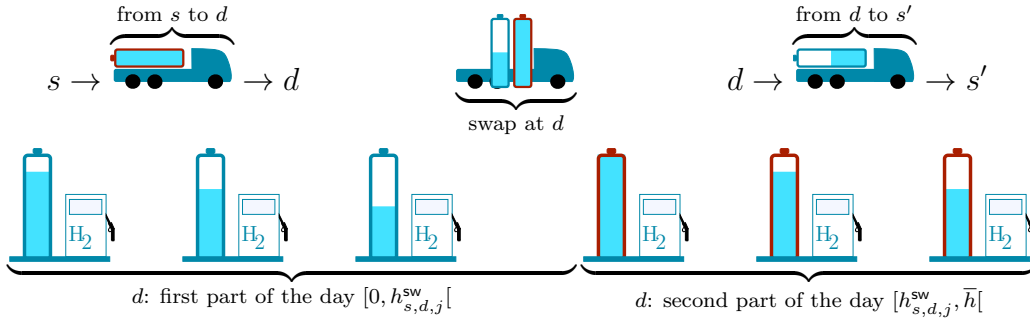


**Figure 2:** The day division at a destination  $d$ : a truck picks up a storage unit from the source  $s$  at  $h_0$ , transports it to the destination  $d$ , performs the swap, and then returns the collected storage unit back to a source  $s'$ . During the first part of the day, the (blue) mobile storage originally located at destination  $d$  satisfies the demand, and during the second part of the day, the newly arrived mobile storage (red) fulfills the demand

follow a back-and-forth structure: storage units depart from the source, reach a destination, and the storage unit previously stationed at that destination immediately returns, rather than forming complete multi-stop tours.

Moreover, in our case, it is the mobile storage units that are transported between locations and that require the monitoring of their stock, making a storage-indexed formulation more appropriate rather than a vehicle-indexed formulation. This approach, however, poses a significant numerical challenge as we expect our model to handle a large number of storage units, and using a storage-indexed formulation leads to an excessive number of variables. In a preliminary study (not described here), we experimented with such formulation but encountered severe computational difficulties due to the presence of symmetrical solutions. For example, if two identical full storage units are available at a source for dispatch, interchanging them does not alter the solution structure or cost, yet it introduces redundancies that

significantly impact solver performance. This issue is further exacerbated as the number of mobile storage units increases, and in the absence of appropriate symmetry-breaking constraints. We refer to the study in [19] for the analysis of MILP models in the presence of symmetries.

To keep the number of variables reasonable and to avoid such symmetries, we propose a *time-expanded* graph reformulation of our problem. This reformulation eliminates the need for mobile storage indexing, thereby breaking some symmetries and is expected to improve numerical resolution. For that purpose, we build from the transport graph a new graph commonly called [12, 16] a *time-expanded graph* (or graph dynamic network flow). The transport of storage unit is replaced by considering both continuous and binary flow variables attached to the arcs of the time-expanded graph and satisfying flow conservation equations (Kirchhoff law) at the graph nodes (to be explained later).

In Sect. 8, we demonstrate how the storage routes (transport planning) can be de-

rived from a solution of the problem on this time-expanded flow graph.

## 4.1 Definition of the time-expanded graph

We turn now to the precise description of the time-expanded graph. In §4.1.1 we define the nodes of the time-expanded graph and in §4.1.2, we define its arcs.

### 4.1.1 Definition of nodes

First, we define the set of nodes of the time-expanded graph. Each node of the expanded graph is an ordered pair composed of a node of the physical transportation graph (source or destination), that is an element of  $\mathcal{V}$ , and of a time index belonging to  $\widehat{\mathbb{J}} = \underline{\mathbb{J}} \cup \overline{\mathbb{J}} \cup \{\overline{0}\}$ . Thus, the set of nodes of the time-expanded graph, denoted as  $\mathcal{V}^{\text{te}}$ , is defined by  $\mathcal{V}^{\text{te}} = \mathcal{V} \times \widehat{\mathbb{J}}$ .

### 4.1.2 Definition of arcs

Second, we define the arcs of the time-expanded graph. The time-expanded graph we build is an oriented multigraph, that is, each edge in the graph is oriented, and two nodes may be connected by more than one oriented edge. As it is used to model physical flows between nodes, an arc is only present between two nodes of  $\mathcal{V}^{\text{te}}$  indexed by two consecutive elements of the time index  $\widehat{\mathbb{J}}$ , that is, between a node  $(v, i)$  and a node  $(v', i^+)$  where  $i^+$  is the successor of  $i \in \widehat{\mathbb{J}}$  (see Equation (1)). For that reason, we only use one time index in an arc specification, that is, the arc  $(v, i) \mapsto (v', i^+)$  in the time-expanded graph is denoted by  $(v, v', i)$  and  $\varphi_{v, v', i}$  when an arc is used as a flow index and a specific notation when two nodes are connected by several arcs as described now.

Since at most one storage unit is transported between a source and a destination (and vice-versa) using Assumption  $A_3$ , and exactly one storage is present at each destination and each time using Assumption  $A_8$ , a single arc  $(v, v', i) = (v, i) \mapsto (v', i^+)$  is sufficient to represent the flow of hydrogen between two nodes  $(v, i)$  and  $(v', i^+)$  of the time-expanded graph for  $(v, v') \in (\mathbb{S} \times \mathbb{D}) \cup \Delta_{\mathbb{D}}$  or  $(v, v') \in (\mathbb{D} \times \mathbb{S}) \cup \Delta_{\mathbb{D}}$ , where  $\mathbb{S} \times \mathbb{D}$  and  $\mathbb{D} \times \mathbb{S}$  correspond to the arcs of the physical graph  $\mathcal{G}$ , and, the addition of  $\Delta_{\mathbb{D}}$  ensures that a storage located at a destination can remain at that destination, while also preventing its transport to a different destination. However, the situation is slightly more complicated when the two involved physical nodes are the same source node, that is  $v = v'$  with  $v \in \mathbb{S}$ . As multiple storage units may remain at a source without being dispatched to a destination, we need several arcs between  $(s, i)$  and  $(s, i^+)$  for  $s \in \mathbb{S}$ . This number of arcs is bounded for each source  $s \in \mathbb{S}$  by the value  $\kappa(s)$  where the function  $\kappa$  is given by Assumption  $A_6$ . Finally, for  $k \in [\kappa(s)]$ , the notation  $(s:k, i)$  denote the  $k$ -th arc  $(s, i) \mapsto (s, i^+)$ . We also use the notation  $\varphi_{s:k, i}$  when a  $k$ -th arc from a source is used as a flow index.

To conclude, the time-expanded graph is defined by  $\mathcal{G}^{\text{te}} = (\mathcal{V}^{\text{te}}, \mathcal{E}^{\text{te}})$ , where the set of nodes  $\mathcal{V}^{\text{te}}$  is  $\mathcal{V} \times \widehat{\mathbb{J}}$  and the set of arcs  $\mathcal{E}^{\text{te}}$  is formally defined as follows:

$$\mathcal{E}^{\text{te}} = \underline{\mathcal{E}} \cup \overline{\mathcal{E}} \cup \widetilde{\mathcal{E}} \quad (2a)$$

$$\text{with } \underline{\mathcal{E}} = ((\mathbb{S} \times \mathbb{D}) \cup \Delta_{\mathbb{D}}) \times \underline{\mathbb{J}}, \quad (2b)$$

$$\overline{\mathcal{E}} = ((\mathbb{D} \times \mathbb{S}) \cup \Delta_{\mathbb{D}}) \times (\overline{\mathbb{J}} \cup \{\overline{0}\}), \quad (2c)$$

$$\widetilde{\mathcal{E}} = \{(s:k) \mid s \in \mathbb{S}, k \in [\kappa(s)]\} \times \widehat{\mathbb{J}}. \quad (2d)$$

The set  $\underline{\mathcal{E}}$  defined in Equation (2b) represents arcs whose first node has its time index in  $\underline{\mathbb{J}}$ , excluding arcs that connect sources

to themselves. The set  $\bar{\mathcal{E}}$  defined in Equation (2c) represents arcs whose first node has its time index in  $\bar{\mathbb{J}} \cup \{0\}$ , excluding arcs that connect sources to themselves. The set  $\tilde{\mathcal{E}}$  defined in Equation (2d) represents arcs that connect each source to itself.

**Definition 1** For an arc  $a \in \mathcal{E}^{\text{te}}$ , we denote by  $t(a) \in \mathcal{V}^{\text{te}}$  its tail node, by  $h(a) \in \mathcal{V}^{\text{te}}$  its head node and by  $d(a) \in \bar{\mathbb{J}}$  the time index of its tail node.

We show in Fig. 3 an example of a time-expanded graph with one source and two destinations, where the arcs belonging to  $\underline{\mathcal{E}}$  are in green, to  $\bar{\mathcal{E}}$  are in red and to  $\tilde{\mathcal{E}}$  are in blue.

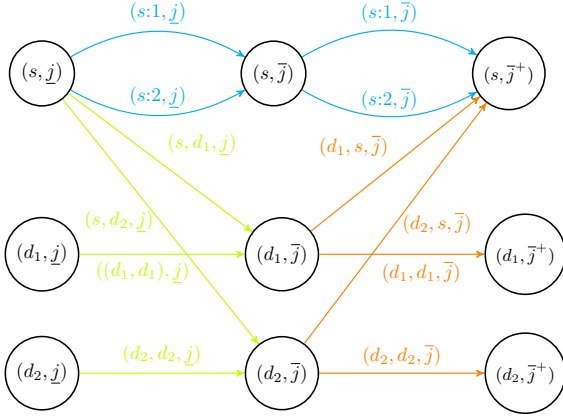


**Figure 3:** Graphic display of a time-expanded graph with one source – where the maximum number of unit storages at source is 2 — and two destinations. The arcs belonging to  $\underline{\mathcal{E}}$  are in green, to  $\bar{\mathcal{E}}$  are in orange and to  $\tilde{\mathcal{E}}$  are in blue

## 4.2 Flows in the time-expanded graph

On the time-expanded graph  $\mathcal{G}^{\text{te}} = (\mathcal{V}^{\text{te}}, \mathcal{E}^{\text{te}})$ , we mainly consider two flows. First, a continuous flow, that we call *hydrogen flow*, which

is a function  $\varphi^{\text{h}} : \mathcal{E}^{\text{te}} \rightarrow [0, \bar{S}]$  which is used to quantify the quantity of hydrogen transported along the arcs, where  $\bar{S}$  represents the maximum possible hydrogen flow, which also corresponds to the maximum capacity of a storage  $\bar{S}$  given by Assumption  $A_1$ . Second, a binary flow, that we call *storage flow*, which is a function  $\varphi^{\text{s}} : \mathcal{E}^{\text{te}} \rightarrow \{0, 1\}$  which is used to detect if a storage is used to transport hydrogen along an arc. For simplicity, for any arc  $a \in \mathcal{E}^{\text{te}}$ , we will denote by  $\varphi_a^{\text{h}}$  (resp.  $\varphi_a^{\text{s}}$ ) the value returned by the function  $\varphi^{\text{h}}$  (resp.  $\varphi^{\text{s}}$ ) for the same arc, that is  $\varphi_a^{\text{h}} = \varphi^{\text{h}}(a)$  (resp.  $\varphi_a^{\text{s}} = \varphi^{\text{s}}(a)$ ). The relationship between the continuous and binary flow will be established in Equation (4).

## 5 Problem modeling on graph $\mathcal{G}^{\text{te}}$

In this section, we model an optimization transport problem on the time-expanded graph and we explicit the constraints on the continuous and binary flow variables at the nodes and on the arcs of the time-expanded graph.

### 5.1 Decision variables

The decision variables are composed on the one hand of the flow decision variables introduced in §4.2 and described in Table 1, and on the other hand of the node decision variables, which are the refilling decisions at the sources and the emptying and swap decisions at the destinations, and which are described in Table 2.

### 5.2 Arc and node constraints

The initial position of the storages on the time-expanded graph  $\mathcal{G}^{\text{te}}$  are part of the data

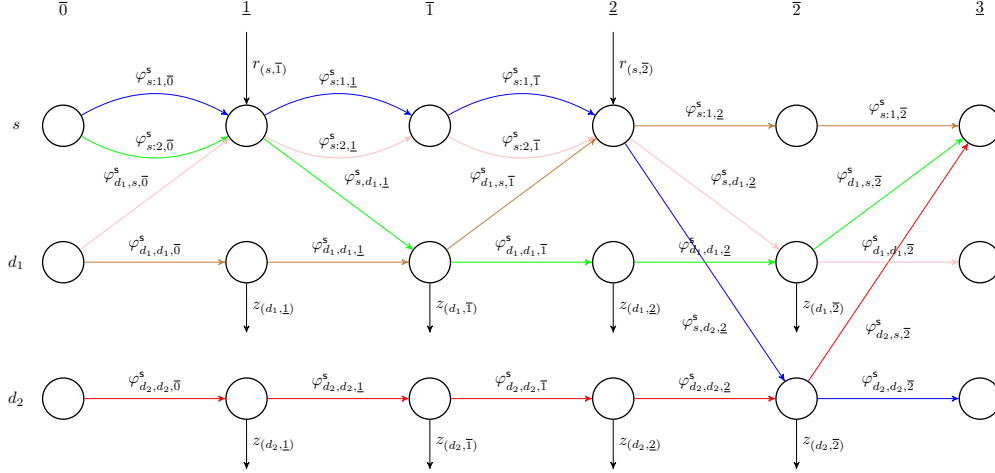


**Figure 4:** Display on a time-expanded graph (with one source, two destinations and an horizon of two days) of a storage flow solution  $\varphi^s$ . We only display the subset of arcs where the storage flow is equal to one. As developed in Sect. 8, transport planning, represented here arc paths (sequence of arcs with the same color), can be derived from  $\varphi^s$ .

Decision	Domain	Description
$\varphi^h = \{\varphi_a^h\}_{a \in \mathcal{E}^{\text{te}}}$	$[0, \bar{S}]^{ \mathcal{E}^{\text{te}} }$	$\varphi_a^h$ is the hydrogen flow in kg circulating on the arc $a \in \mathcal{E}^{\text{te}}$
$\varphi^s = \{\varphi_a^s\}_{a \in \mathcal{E}^{\text{te}}}$	$\{0, 1\}^{ \mathcal{E}^{\text{te}} }$	$\varphi_a^s$ is the storage flow circulating on the arc $a \in \mathcal{E}^{\text{te}}$ .

**Table 1:** Hydrogen and storage flow variables

of the optimization problem. They are given by selecting the active storage flow at time index  $\bar{0}$ . Therefore, the active storage flow at time index  $\bar{0}$  must be equal to the cardinality of the storages set, that is,

$$\sum_{\{a \in \mathcal{E}^{\text{te}} \mid d(a) = \bar{0}\}} \varphi_a^s = |\mathbb{B}|. \quad (3)$$

Here,  $d(a)$  denotes the time index of the starting node of  $a$ , as introduced in Definition 1.

### 5.2.1 Arc constraints

- If there is a positive hydrogen flow on an arc  $a \in \mathcal{E}^{\text{te}}$ , that is, if  $\varphi_a^h > 0$ , then a storage

must be present on the same arc to realize the transport, that is,  $\varphi_a^s = 1$ . Thus the two flows  $\varphi^h$  and  $\varphi^s$  are linked by the following relation

$$\forall a \in \mathcal{E}^{\text{te}}, \varphi_a^h > 0 \implies \varphi_a^s = 1. \quad (4a)$$

If no storage is sent on an arc then, there is no hydrogen flow transported on the same arc, that is,

$$\forall a \in \mathcal{E}^{\text{te}}, \varphi_a^s = 0 \implies \varphi_a^h = 0. \quad (4b)$$

Note that the converse implication does not hold. Indeed, it is possible — and important for returning empty unit storages to sources

Decision	Domain	Description
$z = \{z_{d,i}\}_{(d,i) \in \mathbb{D} \times (\mathbb{J} \cup \bar{\mathbb{J}})}$	$z_{d,i} \in [0, \bar{S}]$	$z_{d,i}$ is the quantity of hydrogen in kg used to satisfy demand at node $(d, i)$
$h^{\text{sw}} = \{h_{s,d,j}^{\text{sw}}\}_{(s,d,j) \in \mathbb{S} \times \mathbb{D} \times \mathbb{J}}$	$h_{s,d,j}^{\text{sw}} \in \mathbb{H}$	$h_{s,d,j}^{\text{sw}}$ is the hour at which swap happens at destination $d$ during day $j \in \mathbb{J}$ for a storage coming from $s$ (arbitrary when no swap)
$r = \{r_{s,j}\}_{(s,j) \in \mathbb{S} \times \bar{\mathbb{J}}}$	$r_{s,j} \in [0, \bar{r}_s]$	$r_{s,j}$ is the quantity of hydrogen in kg used to fill the storages at node $(s, j)$
$\sigma = \{\sigma_{s,j}\}_{(s,j) \in \mathbb{S} \times \bar{\mathbb{J}}}$		$\sigma_{s,j}$ is a bijection of $[ \mathbb{D}  + \kappa(s)]$ used to “follow” storages at sources (see (22)-(23))

**Table 2:** Node variables

— for a storage to be transported on an arc, with  $\varphi_a^s = 1$  with an empty stock  $\varphi_a^h = 0$ .

- For all  $d \in \mathbb{D}$  and for all  $j \in \hat{\mathbb{J}}$ , there must always be exactly one storage at each destination (see Assumption A8)

$$\varphi_{d,d,j}^s = 1. \quad (5)$$

### 5.2.2 Constraints at nodes in $\mathbb{D} \times \bar{\mathbb{J}}$

- For all  $d \in \mathbb{D}$  and all  $j \in \bar{\mathbb{J}}$ , the hydrogen outflow  $\varphi_{d,d,j}^h$  at node  $(d, j)$ , is equal to the hydrogen inflow  $\varphi_{d,d,j}^h$  at the same node, minus the quantity  $z_{d,j}$  used to satisfy the demand during the first part of the day (flow conservation), that is, for all  $d \in \mathbb{D}$  and  $j \in \bar{\mathbb{J}}$

$$\varphi_{d,d,j}^h = \varphi_{d,d,j}^h - z_{d,j}. \quad (6)$$

- For all  $d \in \mathbb{D}$  and  $j \in \bar{\mathbb{J}}$ , the total demand  $D_{d,j}$  at node  $(d, j)$  (total demand at day  $j$  before the swap time), is given by

$$D_{d,j} = \sum_{h \in \mathbb{H}} \mathbf{1}_{\{h\}}(h_{s,d,j}^{\text{sw}}) \times C_{d,j,h}, \quad (7a)$$

$$C_{d,j,h} = \sum_{h'=0}^h q_{d,j,h'}, \quad (7b)$$

where  $q_{d,j,h}$  is the demand at hour  $h$  of day  $j$  at destination  $d$  and  $C_{d,j,h}$  is the cumulative demand from midnight (0) to hour  $h$  of day  $j$  at destination  $d$ .

- For all  $d \in \mathbb{D}$  and  $j \in \bar{\mathbb{J}}$ , the quantity  $z_{d,j}$  used to satisfy the demand at node  $(d, j)$ , is equal to the minimum between the inflow at the same node and the demand, that is,

$$z_{d,j} = \min(\varphi_{d,d,j}^h, D_{d,j}). \quad (8)$$

This ensures that the quantity  $z_{d,j}$  to satisfy the demand is equal to the demand if there is enough hydrogen, otherwise, it is equal to the available hydrogen inflow.

### 5.2.3 Constraints at nodes in $\mathbb{D} \times \bar{\mathbb{J}}$

- For all  $d \in \mathbb{D}$  and for all  $j \in \bar{\mathbb{J}}$ , a node  $(d, j)$  can have at most one positive storage inflow originating from a source node, that is,

$$\sum_{s \in \mathbb{S}} \varphi_{s,d,j}^s \leq 1. \quad (9)$$

- For all  $d \in \mathbb{D}$  and  $j \in \mathbb{J}$ , since the number of positive storage inflows at node  $(d, \bar{j})$  must match the number of positive storage outflows at the same node, it follows that the number of positive storage inflows originating from a source node is equal to the number of positive storage outflows going to a source node (flow conservation), that is,

$$\sum_{s \in \mathbb{S}} \varphi_{s,d,\bar{j}^-}^s = \sum_{s \in \mathbb{S}} \varphi_{d,s,\bar{j}}^s. \quad (10)$$

- For all  $d \in \mathbb{D}$  and  $j \in \mathbb{J}$ , if there is a storage inflow originating from a source at node  $(d, \bar{j}^-)$ , then the hydrogen inflow  $\varphi_{d,d,\bar{j}^-}^h$  will depart to a source node, that is,

$$\varphi_{d,d,\bar{j}^-}^h = \mathbf{1}_{\{0\}} \left( \sum_{s \in \mathbb{S}} \varphi_{s,d,\bar{j}^-}^s \right) \varphi_{d,d,\bar{j}^-}^h + \sum_{s \in \mathbb{S}} \varphi_{d,s,\bar{j}}^h. \quad (11)$$

- For all  $d \in \mathbb{D}$  and  $j \in \mathbb{J}$ , the hydrogen outflow at node  $(d, \bar{j})$ ,  $\varphi_{d,d,\bar{j}}^h$ , is given by

$$\varphi_{d,d,\bar{j}}^h = \sum_{s \in \mathbb{S}} \varphi_{s,d,\bar{j}^-}^h + \mathbf{1}_{\{0\}} \left( \sum_{s \in \mathbb{S}} \varphi_{s,d,\bar{j}^-}^s \right) \varphi_{d,d,\bar{j}^-}^h - z_{d,\bar{j}}. \quad (12)$$

Indeed, if there is a positive hydrogen inflow at node  $(d, \bar{j})$  from a node  $(s', \bar{j}^-)$ , we have that  $\sum_{s \in \mathbb{S}} \varphi_{s,d,\bar{j}^-}^s = 1$  (as the sum is bounded using Equation (9)), which means that a swap happens, that is,  $\varphi_{d,d,\bar{j}}^h = \sum_{s \in \mathbb{S}} \varphi_{s,d,\bar{j}^-}^h - z_{d,\bar{j}} = \varphi_{s',d,\bar{j}^-}^h - z_{d,\bar{j}}$ . Otherwise, if  $\sum_{s \in \mathbb{S}} \varphi_{s,d,\bar{j}^-}^s = 0$ , we have, using Equation (4b), that  $\sum_{s \in \mathbb{S}} \varphi_{s,d,\bar{j}^-}^h = 0$  and that  $\varphi_{d,d,\bar{j}}^h = \varphi_{d,d,\bar{j}^-}^h - z_{d,\bar{j}}$ .

- The swap time at node  $(d, \bar{j})$  equals the departure time  $h_0$  of the storage flow plus the travel time from the source node to the destination node, that is, for all  $s \in \mathbb{S}$  for all  $d \in \mathbb{D}$  and for all  $j \in \mathbb{J}$ , we have

$$\varphi_{s,d,\bar{j}^-}^s = 1 \implies h_{s,d,j}^{\text{sw}} = h_0 + g(s, d). \quad (13)$$

- If no swap occurs at the node, the division of the day  $j$  into its first part  $\bar{j}^-$  and second part  $\bar{j}$  at the same node is made arbitrarily. To reduce symmetry, we set the swap variable to the predetermined value  $(\bar{h} + \underline{h} + 1)/2$ , that is, for all  $d \in \mathbb{D}$  and  $j \in \mathbb{J}$  we have

$$\sum_{s \in \mathbb{S}} \varphi_{s,d,\bar{j}^-}^s = 0 \implies h_{s,d,j}^{\text{sw}} = \frac{\bar{h} + \underline{h} + 1}{2}. \quad (14)$$

- For all  $d \in \mathbb{D}$  and  $j \in \mathbb{J}$ , the total demand  $D_{d,\bar{j}}$  at node  $(d, \bar{j})$  is given by

$$D_{d,\bar{j}} = C_{j,d,\bar{h}} - D_{d,\bar{j}^-}, \quad (15)$$

where  $C_{j,d,\bar{h}}$  is the total demand of day  $j$  at destination  $d$ . From Assumption A<sub>2</sub>, we have that

$$C_{j,d,\bar{h}} \leq \bar{S}.$$

- For all  $d \in \mathbb{D}$  and  $j \in \mathbb{J}$ , the quantity  $z_{d,\bar{j}}$  used to satisfy the demand at node  $(d, \bar{j})$ , is equal to the minimum between the inflow at the same node and demand, that is,

$$z_{d,\bar{j}} = \min(\varphi_{d,d,\bar{j}^-}^h, D_{d,\bar{j}}). \quad (16)$$

#### 5.2.4 Constraints at nodes in $\mathbb{S} \times \underline{\mathbb{J}}$

- For all  $s \in \mathbb{S}$  and for all  $j \in \mathbb{J}$ , the number of positive storage inflows at node  $(s, \underline{j})$  is bounded by the maximum number of storage units that can stay at the source, that is,

$$\sum_{d \in \mathbb{D}} \varphi_{d,s,\underline{j}^-}^s + \sum_{k \in [\kappa(s)]} \varphi_{s:k,\underline{j}^-}^s \leq \kappa(s). \quad (17)$$

- For all  $s \in \mathbb{S}$  and  $j \in \mathbb{J}$ , the number of positive storage inflows at node  $(s, \underline{j})$  is equal to the number of positive storage outflows at the same node (flow conservation), that is,

$$\sum_{d \in \mathbb{D}} \varphi_{d,s,\underline{j}^-}^s + \sum_{k \in [\kappa(s)]} \varphi_{s:k,\underline{j}^-}^s = \sum_{d \in \mathbb{D}} \varphi_{s,d,\underline{j}}^s + \sum_{k \in [\kappa(s)]} \varphi_{s:k,\underline{j}}^s, \quad (18)$$

the initial quantities  $\{\varphi_{d,s,\bar{0}}^s\}_{d \in \mathbb{D}}$  and  $\{\varphi_{s:k,\bar{0}}^s\}_{k \in [\kappa(s)]}$  being given.

- For all  $s \in \mathbb{S}$  and  $j \in \mathbb{J}$ , the hydrogen flow conservation equation is satisfied at each node  $(s, j)$ . The hydrogen inflow plus the refill (which is the quantity of hydrogen purchased at the node), that is, the left-hand side of Equation (19), is equal to the hydrogen outflows at the same node, that is, the right-hand side of Equation (19)

$$\begin{aligned} & \sum_{d \in \mathbb{D}} \varphi_{d,s,\underline{j}}^h + \sum_{k \in [\kappa(s)]} \varphi_{s:k,\underline{j}}^h + r_{s,\underline{j}} \\ &= \sum_{d \in \mathbb{D}} \varphi_{s,d,\underline{j}}^h + \sum_{k \in [\kappa(s)]} \varphi_{s:k,\underline{j}}^h, \end{aligned} \quad (19)$$

the initial quantities  $\{\varphi_{d,s,\bar{0}}^h\}_{d \in \mathbb{D}}$  and  $\{\varphi_{s:k,\bar{0}}^h\}_{k \in [\kappa(s)]}$  being given.

- For all  $s \in \mathbb{S}$  and  $j \in \mathbb{J}$ , the quantity of hydrogen purchased at node  $(s, j)$  is bounded, that is,

$$r_{s,\underline{j}} \leq \bar{r}_s. \quad (20)$$

- For each  $s \in \mathbb{S}$  and each  $j \in \mathbb{J}$ , the stock in all storage units present at source  $s$  must not decrease during the refilling process. Thus, there must exist a bijection which pairs the hydrogen inflows and outflows at source node  $(s, j)$  respecting a non decreasing flow constraint. More formally, to encode this constraint, we fix a source  $s \in \mathbb{S}$  and a day  $j \in \mathbb{J}$  and start by defining two vectors of hydrogen and storage inflows  $\{f_{s,l,\underline{j}}^{\text{in}}\}_{l \in N_s}$  and  $\{y_{s,l,\underline{j}}^{\text{in}}\}_{l \in N_s}$ , where

$$N_s = [|\mathbb{D}| + \kappa(s)], \quad (21)$$

and two vectors of hydrogen and storage outflows  $\{f_{s,l,\underline{j}}^{\text{out}}\}_{l \in N_s}$  and  $\{y_{s,l,\underline{j}}^{\text{out}}\}_{l \in N_s}$  by the follow-

ing equations

$$f_{s,l,\underline{j}}^{\text{in}} = \begin{cases} \varphi_{d_l,s,\underline{j}}^h, & \text{if } l \leq |\mathbb{D}|, \\ \varphi_{s:l-|\mathbb{D}|,\underline{j}}^h, & \text{otherwise,} \end{cases} \quad (22a)$$

$$f_{s,l,\underline{j}}^{\text{out}} = \begin{cases} \varphi_{s,d_l,\underline{j}}^h, & \text{if } l \leq |\mathbb{D}|, \\ \varphi_{s:l-|\mathbb{D}|,\underline{j}}^h, & \text{otherwise,} \end{cases} \quad (22b)$$

$$y_{s,l,\underline{j}}^{\text{in}} = \begin{cases} \varphi_{d_l,s,\underline{j}}^s, & \text{if } l \leq |\mathbb{D}|, \\ \varphi_{s:l-|\mathbb{D}|,\underline{j}}^s, & \text{otherwise,} \end{cases} \quad (22c)$$

$$y_{s,l,\underline{j}}^{\text{out}} = \begin{cases} \varphi_{s,d_l,\underline{j}}^s, & \text{if } l \leq |\mathbb{D}|, \\ \varphi_{s:l-|\mathbb{D}|,\underline{j}}^s, & \text{otherwise,} \end{cases} \quad (22d)$$

for all  $l \in N_s$ , where  $d_l$  is the  $l$ -th destination in the set  $\mathbb{D}$ . Now, we formally define the nondecreasing stock constraint. Let  $A_{s,\underline{j}}$  be the set of active incoming arcs at node  $(s, j)$ , that is  $A_{s,\underline{j}} = \{l \mid y_{s,l,\underline{j}}^{\text{in}} = 1\}$ , and let  $B_{s,\underline{j}}$  be the set of active outgoing arcs at node  $(s, j)$ , that is  $B_{s,\underline{j}} = \{l \mid y_{s,l,\underline{j}}^{\text{out}} = 1\}$ . Note that, the two sets  $A_{s,\underline{j}}$  and  $B_{s,\underline{j}}$  have same cardinality as using (22c), and (22d) and (18) we have

$$|A_{s,\underline{j}}| = \sum_{l \in N_s} y_{s,l,\underline{j}}^{\text{in}} = \sum_{l \in N_s} y_{s,l,\underline{j}}^{\text{out}} = |B_{s,\underline{j}}|.$$

The nondecreasing stock constraint is satisfied if there exists a bijection  $\sigma_{s,\underline{j}} : A_{s,\underline{j}} \rightarrow B_{s,\underline{j}}$  such that

$$f_{s,l,\underline{j}}^{\text{in}} \leq f_{s,\sigma_{s,\underline{j}}(l),\underline{j}}^{\text{out}}, \quad \forall l \in A_{s,\underline{j}}. \quad (23)$$

- For all  $s \in \mathbb{S}$  and  $j \in \mathbb{J}$ , we reduce symmetry in storage flows by imposing to the vector  $\{\varphi_{s:k,\underline{j}}^s\}_{k \in [\kappa(s)]}$  to be nonincreasing, that is, when  $\kappa(s) \geq 2$ , we add for all  $k \in [\kappa(s) - 1]$  the constraint

$$\varphi_{s:k+1,\underline{j}}^s = 1 \implies \varphi_{s:k,\underline{j}}^s = 1. \quad (24)$$

### 5.2.5 Constraints at nodes in $\mathbb{S} \times \bar{\mathbb{J}}$

There is no refill at nodes  $(s, \bar{j})$  as stated in Assumption A<sub>7</sub>, that is, for all  $s \in \mathbb{S}$  and

$j \in \mathbb{J}$

$$\varphi_{s:k,\bar{j}}^h = \varphi_{s:k,\bar{j}}^h, \quad \forall k \in [\kappa(s)], \quad (25a)$$

$$\varphi_{s:k,\bar{j}}^s = \varphi_{s:k,\bar{j}}^s, \quad \forall k \in [\kappa(s)]. \quad (25b)$$

### 5.3 Cost function

We aim at minimizing a cost function which is the addition of four intertemporal costs, namely, a transport cost

$$L^{\text{TR}}(\varphi^s) = c^{\text{TR}} \left( \sum_{(p_1, p_2, i) \in \underline{\mathcal{E}} \cup \bar{\mathcal{E}}} t_{(p_1, p_2)} \times \varphi_{p_1, p_2, i}^s \right), \quad (26a)$$

a refill cost

$$L^{\text{RE}}(r) = \sum_{(s, j) \in \mathbb{S} \times \mathbb{J}} c_s^{\text{RE}} r_{s, \underline{j}}, \quad (26b)$$

a variable demand dissatisfaction cost

$$L^{\text{DV}}(z) = c^{\text{DV}} \left( \sum_{(d, j) \in \mathbb{D} \times \mathbb{J}} (D_{d, \underline{j}} + D_{d, \bar{j}} - (z_{d, \underline{j}} + z_{d, \bar{j}})) \right), \quad (26c)$$

and a fixed demand dissatisfaction cost

$$L^{\text{DF}}(z) = c^{\text{DF}} \left( \sum_{(d, j) \in \mathbb{D} \times \mathbb{J}} \mathbf{1}_{>0} (D_{d, \underline{j}} + D_{d, \bar{j}} - (z_{d, \underline{j}} + z_{d, \bar{j}})) \right), \quad (26d)$$

where  $t_{(p_1, p_2)}$  is the transport time from  $p_1$  to  $p_2$ ,  $c^{\text{TR}}$  is the unit transport cost (€/km),  $c_s^{\text{RE}}$  is the unit purchase price of hydrogen (€/kg) (refilling price) at source  $s$ ,  $c^{\text{DV}}$  is the variable unit dissatisfaction cost (€/kg) and  $c^{\text{DF}}$  is the fixed dissatisfaction cost (€).

## 6 Problem formulation and resolution using MILP and heuristics

### 6.1 Problem formulation

Gathering all that has been done in Sect. 5, we formulate the following optimization problem as follows

$$\begin{aligned} \min_{\varphi^s, \varphi^h, r, z, h^{\text{sw}}, \sigma} \quad & L^{\text{TR}}(\varphi^s) + L^{\text{RE}}(r) \\ & + L^{\text{DV}}(z) + L^{\text{DF}}(z) \quad (27) \\ \text{s.t.} \quad & (4) - (25), \end{aligned}$$

where  $\varphi^s$  and  $\varphi^h$  are the flow decision variables defined in Table 1 and  $r$ ,  $z$ ,  $h^{\text{sw}}$  are respectively the refilling decision at the sources and the emptying and swap decisions at the destinations as defined in Table 2. We denote by  $\text{val}(\mathcal{P})$  the optimal value of Problem (27).

**Lemma 2** *The optimization problem (27), which includes nonlinear constraints—specifically (4), (8), (11), (12), (13), (16), (23), (24)—is equivalent to a MILP, in the sense that the value of the two problems coincide and solutions to either problem can be derived from one another.*

**Proof.** See Appendix A for the proof.  $\square$

Solving the MILP reformulation of Problem (27) is difficult for instances with large number of destinations. This is due to the quadratic growth of the number of variables needed to linearize the nondecreasing stock constraints (23) with respect to the number of destinations. Therefore, using a solver to directly tackle Problem (27) may lead to poor performances. In §6.2.1, we outline the method for solving Problem (27) up to medium-sized instances, and in §6.2.2, we present a heuristic for tackling large-size instances.

## 6.2 Resolution using MILP and heuristics

In §6.2.1, we present the resolution of Problem (27) using a MILP solver, referred to as the MA method. In §6.2.2, we introduce a two-step heuristic approach, that we call the RH method, to address Problem (27), and in §6.2.3, we detail a greedy heuristic, called the GH method, for solving the same problem. The GH method is an improved version of the heuristic employed by the industrial partner for the problem and will serve as a baseline for comparison against MA and RH.

In all the three presented algorithms a MILP solver, specifically Gurobi, is used as a core ingredient. It is executed with a predefined time limit, which is the same for all the three algorithms, to prevent excessive computational time and ensure practical applicability of the proposed algorithms, and to ensure a fair comparison of the three algorithms. It is important to note that the time limit imposed on the two-step heuristic is only applied to its first step, as the second step executes rapidly, as detailed in the corresponding section.

### 6.2.1 MILP resolution of Problem (27)

Problem (27), which is equivalent to a MILP (see Lemma 2), is solved using a MILP solver (Gurobi), without employing any additional techniques or improvements. For medium-sized instances, Gurobi demonstrates strong performance and produces high-quality results. However, its effectiveness diminishes when applied to large-scale instances. The medium-sized instances considered in this study include up to 35 destinations. In what follows, we will refer to the direct use of Gurobi to solve Problem (27) as MA.

### 6.2.2 Resolution of Problem (27) using a two-step heuristic

Using a MILP solver to directly tackle Problem (27) may lead to poor performances for large instances due to the nondecreasing stock constraint (23), which is highly combinatorial.

For that reason, when considering large instances of Problem (27), we rely on a heuristic, that we call RH. Before describing this heuristic, we consider two additional optimization problems. The first one is the same optimization problem as Problem (27), but without the permutation constraint (23), that is,

$$\begin{aligned} \min_{\varphi^s, \varphi^h, r, z, h^{sw}, \sigma} & L^{\text{TR}}(\varphi^s) + L^{\text{RE}}(r) \\ & + L^{\text{DV}}(z) + L^{\text{DF}}(z) \quad (28) \\ \text{s.t.} & (4)–(20), (24), (25) . \end{aligned}$$

We denote by  $\text{val}(\tilde{\mathcal{P}})$  the optimal value of Problem (28). Since the feasible set of Problem (27) is included in feasible set of Problem (28), we have that

$$\text{val}(\tilde{\mathcal{P}}) \leq \text{val}(\mathcal{P}) . \quad (29)$$

Consequently, a lower bound of Problem (28) is also a lower bound for Problem (27).

The second optimization problem is an equivalent formulation of Problem (27), which is given by

$$\begin{aligned} \min_{\varphi^s} & L^{\text{TR}}(\varphi^s) + \phi(\varphi^s) \quad (30) \\ \text{s.t.} & (5), (9), (10), (17), (18), (24) , \end{aligned}$$

where the function  $\phi(\varphi^s)$  is the optimal value of

$$\begin{aligned} \min_{\varphi^h, r, z, h^{sw}, \sigma} & L^{\text{RE}}(r) + L^{\text{DV}}(z) + L^{\text{DF}}(z) \quad (31) \\ \text{s.t.} & (4), (6)–(8), (11)–(16), \\ & (19)–(23), (25) . \end{aligned}$$

We also denote by  $\gamma(\varphi^s)$  the optimal solution of Problem (31). Given a feasible storage flow  $\varphi^s$ , that is, a storage flow  $\varphi^s$  satisfying the constraints of Problem (30), computing the value of  $\phi(\varphi^s)$  amounts to solve Problem (31) on the subgraph of  $\mathcal{G}^{\text{te}}$  generated by active arcs of  $\varphi^s$ , which is a MILP with much fewer integer variables than in Problem (27) as we only consider the nondecreasing stock constraint (23) on this subgraph. As a consequence, computing  $\phi(\varphi^s)$  is tractable even for large-size instances.

Now, we detail the RH method to solve large-sized instances of Problem (30). First, note that solving Problem (28) is easier than Problem (27) since it does not include the nondecreasing stock constraint (23). Second, for a feasible solution  $\varphi^s$  of Problem (28), that is, for a solution  $\varphi^s$  that satisfies Constraints (5), (9), (10), (17), (18) and (24), solving Problem (31) is easy as previously mentioned, and the whole solution  $(\varphi^s, \gamma(\varphi^s))$  is feasible for the original Problem (27) as  $\varphi^s$  is feasible for Problem (30) and  $\gamma(\varphi^s)$  is feasible for Problem (31). Therefore, the heuristic approach first solves Problem (28) with a computation time limit to obtain a feasible storage flow  $\varphi^s$ , and then, solves Problem (31) to obtain a feasible solution for Problem (27). For what follows, we refer to the lower bound obtained by RH as the lower bound obtained when solving Problem (28) in the first step of the heuristic. A short pseudocode for RH is given in Algorithm 1

Surprisingly, RH yields better results compared to using MA for large instances. It also produces tighter lower bounds, which facilitates verifying the near-optimality of the solutions found.

**Remark 3** *One might consider applying Benders decomposition to Problem (30) by approximating the function  $\phi$  using a set*

*of cuts. However, as demonstrated in the numerical results section, the RH method is enough to obtain high-quality solutions to Problem (27). Moreover, the nonconvexity of  $\phi$  with respect to  $\varphi^s$ , as Problem (31) involves binary variables, makes the application of Benders decomposition more challenging. Although some techniques have been proposed to handle such nonconvexity in the context of Benders decomposition [13], there is no guarantee that they will be effective for Problem (30).*

### 6.2.3 A greedy heuristic for Problem (27)

We introduce a third approach — which is an improved version of the heuristic employed by the industrial partner for the problem —, that we will call GH, to serve as a baseline for comparison against the methods described in §6.2.1 and in §6.2.2. While GH is suboptimal, it provides solutions that are fast to compute.

In Algorithm 2, we present the pseudocode of GH, which is composed of two steps. First, it finds a feasible storage flow  $\varphi^s$  to Problem (30) and, second, solves Problem (31) (which is a tractable MILP as already explained) to obtain a feasible solution  $(\varphi^s, \gamma(\varphi^s))$  to the global Problem (27).

During the first step, it is assumed that the sources have sufficient refilling capacity to fully replenish the storages. More precisely, for a given day  $j$ , if a storage is sent from a source  $s$  to a destination  $d$ , that is, if  $\varphi_{s,d,j}^s$  is set to the value 1, then the storage is sent full, that is,  $\varphi_{s,d,j}^h$  is set to the value  $\bar{S}$ . This assumption may violate constraints (19) and (20) but at the end of the first step, the intermediate hydrogen flow  $\varphi^h$  is not kept and it is recomputed when solving Problem (31).

---

**Algorithm 1** Two-step heuristic (RH) for Problem (27)

---

- 1: Solve Problem (28) with a time limit to obtain  $\varphi^s$
  - 2: Solve Problem (31) to obtain  $\gamma(\varphi^s)$
  - 3: **return**  $(\varphi^s, \gamma(\varphi^s))$
- 

Now, we detail the first step. We sequentially iterate on the set  $\mathbb{J}$  of days, to build an admissible storage flow  $\varphi^s$  together with a compatible hydrogen flow  $\varphi^h$  as follows.

1. At the start of day  $j \in \mathbb{J}$ , having already computed  $\varphi^s$  and  $\varphi^h$  for the previous days, we compute a subset of destinations  $\mathbb{D}^{\text{CR}} = \{d \in \mathbb{D} \mid \varphi_{d,d,j}^h \leq S^{\text{CR}}\}$ , referred to as the *critical destinations*, whose hydrogen inflow  $\varphi_{d,d,j}^h$  have fallen below a predefined threshold  $S^{\text{CR}}$ . The destinations belonging to the subset  $\mathbb{D}^{\text{CR}}$  are selected for replenishment and are sorted in ascending order with respect to their hydrogen inflow.
2. Then, we iterate on the ordered critical destinations as follows. The closest source to the current destination with available storages is selected and one of its storages is sent (full, according to previous assumption made) to the current destination and removed from the available storages. The storage that was already present at the destination is returned to the same source and will be available the next day.
3. The iteration on the ordered critical destinations for the current day stops when all the ordered critical destinations have been served or if there is no more available storages at the sources.
4. Finally, the hydrogen flow  $\varphi^h$  for day  $j$  is updated using Equations (6) and (12).

## 7 Computational experiments

We aim to analyze the quality of the solutions for Problem (27) provided by the three methods previously introduced, namely MA (in §6.2.1), RH (in §6.2.2) and GH (in §6.2.3).

### 7.1 Experimental Setting

#### 7.1.1 Instances

We describe now the set of instances used for numerical tests. We vary the number of sources, destinations, and storages – to reflect both what is found in the current infrastructure and what will be found in anticipated possible expansions – together with their characteristics and transport characteristics.

Each instance is characterized by its number of sources, number of destinations, number of storages, demand profile magnitude and dissatisfaction cost magnitude for a total of 192 instances. The difficulty of an instance is mainly driven by its number of locations and more precisely its number of destinations, as it will be discussed later. We describe now more precisely how the different parameters vary in the instances.

- Characteristics of the sources
  - The number of sources ranges from 1 to 7, that is  $1 \leq |\mathbb{S}| \leq 7$ .
  - The refilling capacity and price at each source are given in Table 3.

---

**Algorithm 2** Greedy heuristic (GH) for Problem (27)
 

---

**Input:** parameter  $S^{\text{CR}}$  ▷ the critical stock threshold  
 1: **for**  $j = 1, \dots, J$  **do**  
 2:   **for**  $s \in \mathbb{S}$  **do**  
 3:      $V[s] \leftarrow \sum_{d \in \mathbb{D}} \varphi_{d,s,\bar{j}-1}^s + \sum_{k \in [\kappa(s)]} \varphi_{s:k,\bar{j}-1}^s$  ▷ number of available storages at  $s$  the day  $j$   
 4:   **end for**  
 5:    $\mathbb{D}^{\text{CR}} \leftarrow \{d \in \mathbb{D} \mid \varphi_{d,d,\bar{j}}^h \leq S^{\text{CR}}\}$  ▷ Initialize the critical destinations  
 6:   Sort  $\mathbb{D}^{\text{CR}}$  in ascending order of  $\varphi_{d,d,\bar{j}}^h$   
 7:   **for**  $d \in \mathbb{D}^{\text{CR}}$  **do**  
 8:      $s' \leftarrow \arg \min_{\substack{s \in \mathbb{S} \\ V[s] \geq 1}} g(s, d)$  ▷ Select the closest source with available storages  
 9:     **if**  $s' = \emptyset$  **then** break  
 10:    **end if**  
 11:      $\varphi_{s',d,\bar{j}}^s \leftarrow 1$  ▷ Send the full storage from  $s'$  to  $d$   
 12:      $V[s'] \leftarrow V[s'] - 1$  ▷ Decrease the number of available storages at  $s'$   
 13:      $\varphi_{d,s',\bar{j}}^s \leftarrow 1$  ▷ Return the storage from  $d$  back to the same source  $s'$   
 14:     Update  $\varphi^h$  using Equations (6) and (12)  
 15:    **end for**  
 16: **end for**  
 17: Compute  $\gamma(\varphi^s)$  ▷  $\gamma(\varphi^s)$  is the optimal solution of Problem (31)  
 18: **return**  $(\varphi^s, \gamma(\varphi^s))$

---

Source	Refilling capacity $\bar{r}_s$	Refilling price $c_s^{\text{RE}}$
$s_1$	1300	9.0
$s_2$	1500	8.0
$s_3$	1700	8.3
$s_4$	1000	8.0
$s_5$	1000	8.0
$s_6$	800	10.0
$s_7$	500	7.0

**Table 3:** Refilling capacity and price of the sources, where  $s_l$  is the  $l$ -th source of  $\mathbb{S}$ .

- The maximum number  $\kappa(s)$  of storages that can be present at source  $s$ , is equal to 4, for all  $s \in \mathbb{S}$ .
- Characteristics of the destinations
  - The ratio  $|\mathbb{D}|/|\mathbb{S}|$  ranges from 4.33 to 8.5.
  - Demand follows a three-peaked daily pattern, with peaks at 8:00, 14:00, and 17:00. On Saturdays and Sundays, demand reduces to 50% and 25%, respectively, of the weekday level.
  - Each instance is characterized by a demand profile magnitude and a demand dissatisfaction cost magnitude. There are two types of the demand profile magnitude. For first one, the average weekday demand at each destination is 85 kg per day. For the second one, the average weekday demand at each destination is 130 kg per day. In Figure 5, we show an example of a demand profile for a weekday at a destination with an average daily demand of 85 kg. There are also two types of the demand dissatisfaction cost magnitude. For the first

one, the variable demand dissatisfaction cost  $c^{\text{DV}}$  is equal to 12€/kg, and the fixed demand dissatisfaction cost  $c^{\text{DF}}$  is equal to 1,500€. For the second one, the variable demand dissatisfaction cost,  $c^{\text{DV}}$ , is equal to 14€/kg and the fixed demand dissatisfaction cost,  $c^{\text{DF}}$ , is equal to 2,500€.

- The swap time at the destinations is equal to 1 hour.
- Characteristics of the storages
  - The maximal stock capacity  $\bar{S}$  of the storages is equal to 300 kg.
  - The ratio  $|\mathbb{B}|/|\mathbb{D}|$  ranges from 1.26 to 1.5.
  - The stock capacity at the beginning of the time span of the storages that are located at the source is equal to 200 kg.
  - The stock capacity at the beginning of the time span of the storages that are located at the destinations is equal to 200 kg.
- Characteristics of the transport
  - The distances between the sources and the destinations are randomly generated within a range of 1 km to 123 km, based on the values of the case study. Specifically, for all  $(p_1, p_2) \in (\mathbb{S} \times \mathbb{D}) \cup (\mathbb{D} \times \mathbb{S})$ , we have that  $1 \leq t_{(p_1, p_2)} = t_{(p_2, p_1)} \leq 123$ .
  - The transport cost  $c^{\text{TR}}$  is equal to 2.25€/km.
  - The trucks arrive at  $h_0 = 8$  at the sources to transport the storages.

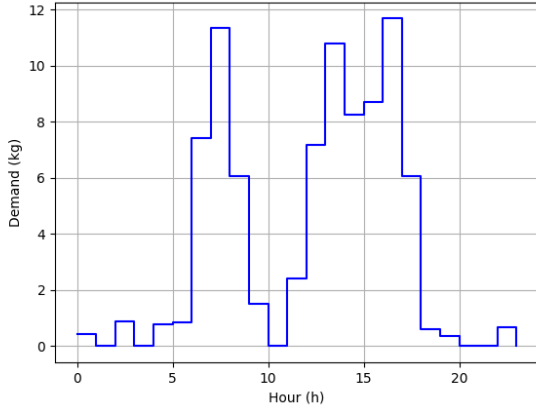


**Figure 5:** Example of a demand profile for a weekday at a destination with an average daily demand of 85 kg

### 7.1.2 Implementation

The MILP model is implemented in Julia 1.9.2. using JuMP [18] as the modeler and Gurobi 11.0 [14] as the MILP solver. All computations were performed on a Linux system equipped with 4-processor Intel Xeon E5-2667, 3.30GHz, with 192 GB of RAM. For each instance and for each algorithm, the maximum execution time is set to 20 min (GH method finishes way before this time limit)

## 7.2 Performance analysis

### 7.2.1 Total cost comparison

The most straightforward metric for evaluating our algorithms is the cost function of Problem (27) that is being minimized. In Figure 6, we show the cost obtained by each algorithm over the whole instances summarized as boxplots. The red line (resp. the purple triangle) indicates the median (resp. the mean) over the instances, the ends of the boxes the first and third quartiles. The whiskers extend to either 1.5 times the interquartile range (the

difference between the third and first quartiles) or the last data point within this range, whichever is closer, and any points beyond are considered outliers.

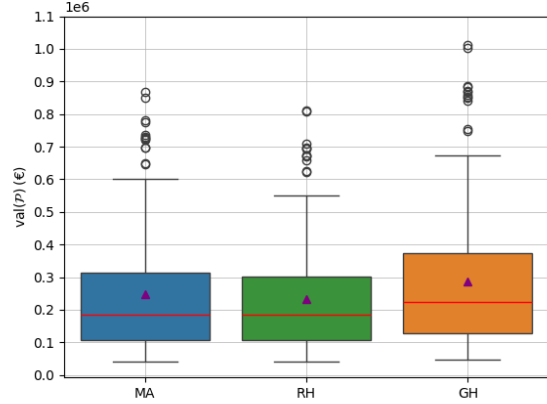


**Figure 6:** Cost obtained by each algorithm over the whole instances summarized as boxplots, where the lower the mean (represented by the purple triangle) the better

**Result 1** *The best solution given by the MA and RH methods is always better than the solution returned by the GH method for all the instances. Moreover, the median (resp. the mean) obtained by the MA and RH methods outperform the median (resp. the mean) obtained by the GH method by 17.7% and 17.8% (resp. 14.1% and 18.9%).*

### 7.2.2 Total cost comparison per number of destinations

As shown in Figure 6, there is a slight difference between the cost distribution returned by MA and by RH and, as previously mentioned, we expect RH to perform better on large instances. To investigate this, we assign to each instance an indicator, that we call  $Q_{-destination}$ , based on its number of destinations. This indicator takes four distinct

values, ranging from  $Q_1$  to  $Q_4$ , following the classification criteria outlined in Table 4. For example, an instance is assigned the value  $Q_2$  if its number of destinations falls within the range of 19 to 27. Note that the threshold values in Table 4 are selected to ensure an equal distribution of instances across all the indicator values, resulting in exactly 48 instances per category.

Q_destination	$ \mathbb{D} $
$Q_1$	[10,18]
$Q_2$	[19,27]
$Q_3$	[28,35]
$Q_4$	[36,48]

**Table 4:** Threshold values defining the classification of instances according to their number of destinations.

In Figure 7, we show the cost obtained by each algorithm over the whole instances summarized as boxplots, with an additional partitioning using the indicator Q\_destination.

**Result 2** *The MA and RH methods show comparable performance for the first three values of the indicator Q\_destination, that is  $Q_1$ ,  $Q_2$  and  $Q_3$ . However, for the value  $Q_4$ , the median (resp. the mean) obtained by the RH algorithm outperforms the median (resp. the mean) obtained by the MA algorithm by 12.7% (resp. 9%).*

### 7.2.3 Relative gap comparison per number of destinations

For a given algorithm, the relative gap of an instance is defined as the difference between an upper bound given by the value of the best solution and a lower bound returned by the algorithm, divided by the same upper bound.

We show in Figure 8 the relative gap obtained by MA and RH algorithms over the

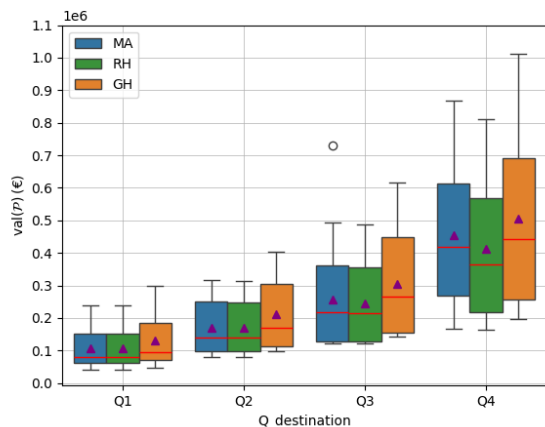


**Figure 7:** Cost obtained by each algorithm over the whole instances summarized as boxplots, along with an additional partitioning using the indicator Q\_destination, where a higher value of this indicator corresponds to a higher number of destinations

whole instances summarized as boxplots, with an additional partitioning using the indicator Q\_destination.

**Result 3** *The relative gap of the MA algorithm increases significantly as the number of destinations grows, reducing its ability to effectively determine the quality of the solution. This relative gap for  $Q_4$  is equal to 23.9% in median and 26.4% in average. In contrast, the lower bounds found using the RH algorithm are tighter, with a relative gap for  $Q_4$  equals to 5% in median and 7.7% in average.*

### 7.2.4 Relative gap comparison according to the demand satisfaction

For each instance, we introduce an indicator called  $S\_demand$ , which takes the value “yes” if all the demands at the destinations are satisfied, and “no” otherwise. Then, we present in Figure 9 the relative gap obtained by MA and RH algorithms over the whole instances

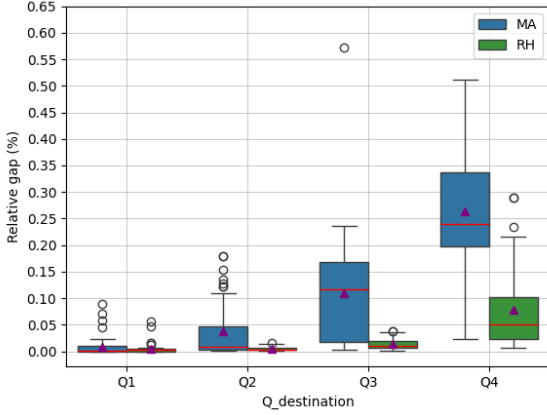


**Figure 8:** Relative gap obtained by MA and RH algorithms over the whole instances summarized as boxplots, along with an additional partitioning using the indicator  $Q\_destination$  given in Table 4

summarized as boxplots, with an additional partitioning using the indicator  $S\_demand$ .

**Result 4** *When the best solution found fully satisfies the demand, both algorithms find tight lower bound that guarantee the near-optimality of the solution. However, when the demand is not fully satisfied, RH's ability to determine whether the solution is optimal decreases slightly, while the relative gap produced by MA increases significantly. In other words, if the MA's best solution fails to satisfy all the demands, near-optimality of the solution is not guaranteed.*

## 8 From flow to storage transport planning

In this section, we show in Proposition 9 how to derive a transport planning for all storages  $b \in \mathbb{B}$  given a solution of Problem (27). In order to prove Proposition 9, we start by notations and preliminary result.

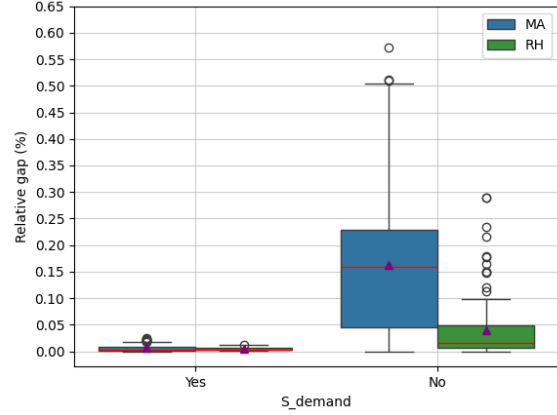


**Figure 9:** Relative gap obtained by MA and RH algorithms over the whole instances summarized as boxplots, along with an additional partitioning using the indicator  $S\_demand$

**Lemma 4** *Given an admissible solution of Problem (27), for all  $s \in \mathbb{S}$  and all  $\underline{j} \in \underline{\mathbb{J}}$ , we can extend the bijection  $\sigma_{s,\underline{j}} : A_{s,\underline{j}} \rightarrow B_{s,\underline{j}}$  to a bijection  $\bar{\sigma}_{s,\underline{j}} : N_s \rightarrow N_s$ , which satisfies*

$$y_{s,l,\underline{j}}^{\text{in}} = y_{s,\bar{\sigma}_{s,\underline{j}}(l),\underline{j}}^{\text{out}}, \quad \forall l \in N_s. \quad (32)$$

**Proof.** We fix  $s \in \mathbb{S}$  and  $\underline{j} \in \underline{\mathbb{J}}$ . As  $|A_{s,\underline{j}}| = |B_{s,\underline{j}}|$ , the set of bijections from  $N_s \setminus A_{s,\underline{j}}$  to  $N_s \setminus B_{s,\underline{j}}$  is nonempty and we pick one such bijection  $\tilde{\sigma}_{s,\underline{j}} : N_s \setminus A_{s,\underline{j}} \rightarrow N_s \setminus B_{s,\underline{j}}$ . Defining  $\bar{\sigma}_{s,\underline{j}}$  by

$$\bar{\sigma}_{s,\underline{j}}(l) = \begin{cases} \sigma_{s,\underline{j}}(l) & \text{if } l \in A_{s,\underline{j}}, \\ \tilde{\sigma}_{s,\underline{j}}(l) & \text{if } l \in N_s \setminus |A_{s,\underline{j}}|, \end{cases} \quad (33)$$

it is straightforward to see that (32) is satisfied as storage flows of value 1 are propagated by  $\sigma_{s,\underline{j}}$  and storage flows of value 0 are propagated by  $\tilde{\sigma}_{s,\underline{j}}$ .  $\square$

Now, we introduce some notations. For all  $\underline{j} \in \underline{\mathbb{J}}$ , we consider the mappings  $\theta_{\underline{j}}$  defined as

follows

$$\theta_{\underline{j}} : \mathcal{E}_{\underline{j}^-}^{\text{te}} \rightarrow \mathcal{E}_{\underline{j}}^{\text{te}}$$

$$(s:k, \underline{j}^-) \mapsto \begin{cases} (s, d_{\nu}, \underline{j}) & \text{if } l' \leq |\mathbb{D}| \\ (s, l' - |\mathbb{D}|, \underline{j}) & \text{otherwise} \\ \text{with } l' = \bar{\sigma}_{s, \underline{j}}(k + |\mathbb{D}|) \end{cases} \quad (34a)$$

$$(d_l, s, \underline{j}^-) \mapsto \begin{cases} (s, d_{\nu}, \underline{j}) & \text{if } l' \leq |\mathbb{D}| \\ (s, l' - |\mathbb{D}|, \underline{j}) & \text{otherwise} \\ \text{with } l' = \bar{\sigma}_{s, \underline{j}}(l) \end{cases} \quad (34b)$$

$$(d, d, \underline{j}^-) \mapsto (d, d, \underline{j}), \quad (34c)$$

where, for all  $\underline{j} \in \widehat{\mathbb{J}}$ , the subset of arcs  $\mathcal{E}_{\underline{j}}^{\text{te}}$  is defined by  $\mathcal{E}_{\underline{j}}^{\text{te}} = \{a \in \mathcal{E}^{\text{te}} \mid \mathbf{d}(a) = \underline{j}\}$ , where  $\mathbf{d}$  was defined in §4.1.2.

**Lemma 5** *For all  $\underline{j} \in \mathbb{J}$ , the mapping  $\theta_{\underline{j}}$  defined in Equation (34) is well-defined, satisfies  $\mathbf{t}(\theta_{\underline{j}}(a)) = \mathbf{h}(a)$  and is bijective. Moreover, it preserves the value of the storage flow as we have  $\varphi_a^s = \varphi_{\theta_{\underline{j}}(a)}^s$  for all  $a \in \mathcal{E}_{\underline{j}^-}^{\text{te}}$ .*

**Proof.** The mapping  $\theta_{\underline{j}}$  is well-defined, as by construction it maps each element of  $\mathcal{E}_{\underline{j}^-}^{\text{te}}$  to a corresponding element in  $\mathcal{E}_{\underline{j}}^{\text{te}}$ . From the definition in Equation (34) of the mapping  $\theta_{\underline{j}}$ , it is straightforward to check that  $\mathbf{t}(\theta_{\underline{j}}(a)) = \mathbf{h}(a)$  for any  $a \in \mathcal{E}_{\underline{j}^-}^{\text{te}}$ . Furthermore,  $\theta_{\underline{j}}$  is bijective, as the underlying mapping  $\bar{\sigma}_{s, \underline{j}}$  built in Lemma 4 is itself bijective.

Now, we check that the storage flows are preserved. First, if  $a = (s:k, \underline{j}^-)$  or  $a = (d_l, s, \underline{j}^-)$ , we have that  $\varphi_a^s = \varphi_{\theta_{\underline{j}}(a)}^s$  using Equation (32). Second, if  $a = (d, d, \underline{j}^-)$ , the equality  $\varphi_a^s = \varphi_{\theta_{\underline{j}}(a)}^s$  is satisfied using Equation (5) which gives that  $\varphi_a^s$  and  $\varphi_{\theta_{\underline{j}}(a)}^s$  are both equal to one which ends the proof.  $\square$

For  $\bar{j} \in \bar{\mathbb{J}}$ , we consider the mappings  $\theta_{\bar{j}}$  defined as follows

$$\theta_{\bar{j}} : \mathcal{E}_{\bar{j}^-}^{\text{te}} \rightarrow \mathcal{E}_{\bar{j}}^{\text{te}}$$

$$(s:k, \bar{j}^-) \mapsto (s:k, \bar{j}) \quad (35a)$$

$$(s, d, \bar{j}^-) \mapsto \begin{cases} (d, d, \bar{j}) & \text{if } \varphi_{s, d, \bar{j}^-}^s = 1 \\ (d, \hat{\sigma}_{d, \bar{j}}(s), \bar{j}) & \text{otherwise} \end{cases} \quad (35b)$$

$$(d, d, \bar{j}^-) \mapsto \begin{cases} (d, s, \bar{j}) & \text{if } \exists s \text{ s.t. } \varphi_{d, s, \bar{j}}^s = 1 \\ (d, d, \bar{j}) & \text{otherwise,} \end{cases} \quad (35c)$$

where  $\hat{\sigma}_{d, \bar{j}}$  is any bijection from the subset  $\{s \in \mathbb{S} \mid \varphi_{s, d, \bar{j}^-}^s = 0\}$  to the subset  $\{s \in \mathbb{S} \mid \varphi_{d, s, \bar{j}}^s = 0\}$ , which is guaranteed to exist as the two subsets  $\{s \in \mathbb{S} \mid \varphi_{s, d, \bar{j}^-}^s = 0\}$  and  $\{s \in \mathbb{S} \mid \varphi_{d, s, \bar{j}}^s = 0\}$  have the same cardinality using Equation (10).

**Lemma 6** *For  $\bar{j} \in \bar{\mathbb{J}}$ , the mapping  $\theta_{\bar{j}}$  defined in Equation (35) is well-defined, bijective and satisfies  $\mathbf{t}(\theta_{\bar{j}}(a)) = \mathbf{h}(a)$ . Moreover, it preserves the value of the storage flow as we have  $\varphi_a^s = \varphi_{\theta_{\bar{j}}(a)}^s$  for all  $a \in \mathcal{E}_{\bar{j}^-}^{\text{te}}$ .*

**Proof.** The mapping  $\theta_{\bar{j}}$  is well-defined, as by construction it maps each element of  $\mathcal{E}_{\bar{j}^-}^{\text{te}}$  to a corresponding element in  $\mathcal{E}_{\bar{j}}^{\text{te}}$ . From the definition in Equation (35) of the mapping  $\theta_{\bar{j}}$ , it is straightforward to check that  $\mathbf{t}(\theta_{\bar{j}}(a)) = \mathbf{h}(a)$  for any  $a \in \mathcal{E}_{\bar{j}^-}^{\text{te}}$ . Now, we turn to the proof that the mapping  $\theta_{\bar{j}}$  is bijective. Since both the domain and codomain of  $\theta_{\bar{j}}$  have the same cardinality, that is  $|\mathcal{E}_{\bar{j}^-}^{\text{te}}| = |\mathcal{E}_{\bar{j}}^{\text{te}}|$  it is enough to prove that  $\theta_{\bar{j}}$  is surjective to obtain that it is bijective. To prove that  $\theta_{\bar{j}}$  is surjective we proceed by cases in the arc set  $\mathcal{E}_{\bar{j}}^{\text{te}}$ .

- First, for an arc of the form  $(s:k, \bar{j})$ , it follows directly from Equation (35a) that  $\theta_{\bar{j}}((s:k, \bar{j}^-)) = (s:k, \bar{j})$ .

- Second, for an arc  $(d, d, \bar{j})$ , we have to consider two possibilities. If there exists  $s \in \mathbb{S}$  such

that  $\varphi_{s,d,\bar{j}^-}^s = 1$ , then  $\theta_{\bar{j}}((s,d,\bar{j}^-)) = (d,d,\bar{j})$  using Equation (35b). Otherwise, we have that  $\varphi_{s,d,\bar{j}^-}^s = 0$  for all  $s \in \mathbb{S}$  and it follows using Equation (10) that  $\varphi_{d,s,\bar{j}}^s = 0$  for all  $s \in \mathbb{S}$  and therefore that  $\theta_{\bar{j}}((d,d,\bar{j}^-)) = (d,d,\bar{j})$  using Equation (35c).

• Third, for an arc of the form  $(d,s,\bar{j})$ , we have again to consider two possibilities. If  $\varphi_{d,s,\bar{j}}^s = 1$ , then  $\theta_{\bar{j}}((d,d,\bar{j}^-)) = (d,s,\bar{j})$  using Equation (35c). Otherwise, by definition of  $\hat{\sigma}_{\bar{j},d}$ , there exists  $s'$  such that  $\hat{\sigma}_{\bar{j},d}(s') = s$ , and therefore we have using Equation (35b) that  $\theta_{\bar{j}}((s',d,\bar{j}^-)) = (d,\hat{\sigma}_{\bar{j},d}(s'),\bar{j}) = (d,s,\bar{j})$ .

We conclude that all the arcs in  $\mathcal{E}_{\bar{j}}^{\text{te}}$  are in the image of  $\theta_{\bar{j}}$  and thus  $\theta_{\bar{j}}$  is surjective.

It remains to prove that  $\theta_{\bar{j}}(a)$  preserves the value of the storage flow. We consider the three possible cases enumerated in Equation (35).

1. If  $a = (s:k,\bar{j}^-)$ , we have

$$\varphi_a^s = \varphi_{s:k,\bar{j}^-}^s = \varphi_{s:k,\bar{j}}^s = \varphi_{\theta_{\bar{j}}(a)}^s$$

using Equation (25) and Equation (35a).

2. If  $a = (s,d,\bar{j}^-)$  we have two subcases to consider. If  $\varphi_a^s = 1$  then we have

$$\varphi_a^s = \varphi_{s,d,\bar{j}^-}^s = 1 = \varphi_{d,d,\bar{j}}^s = \varphi_{\theta_{\bar{j}}(a)}^s,$$

using Equation (5) and Equation (35b). Otherwise, we have

$$\varphi_a^s = \varphi_{s,d,\bar{j}^-}^s = \varphi_{d,\hat{\sigma}_{d,\bar{j}}(s),\bar{j}}^s = \varphi_{\theta_{\bar{j}}(a)}^s,$$

using the definition of  $\hat{\sigma}_{d,\bar{j}}$  and Equation (35b).

3. If  $a = (d,d,\bar{j}^-)$ , we again consider two subcases. If there exists  $s$  such that  $\varphi_{d,s,\bar{j}}^s = 1$ , we obtain

$$\varphi_a^s = \varphi_{d,d,\bar{j}^-}^s = 1 = \varphi_{d,s,\bar{j}}^s = \varphi_{\theta_{\bar{j}}(a)}^s,$$

using Equation (5) and Equation (35c). Otherwise, we have that

$$\varphi_a^s = \varphi_{d,d,\bar{j}^-}^s = 1 = \varphi_{d,d,\bar{j}}^s = \varphi_{\theta_{\bar{j}}(a)}^s,$$

using Equation (5) and Equation (35c).

Thus, in all cases,  $\theta_{\bar{j}}$  preserves the value of the storage flow which concludes the proof.  $\square$

We prove in Lemma 7 that the number of active storage flows for each day is constant and equal to the number of storages  $|\mathbb{B}|$ . This result serves as a control test, as our flow formulation is designed to ensure that the number of active storage flows is globally conserved.

**Lemma 7** For all  $j \in \hat{\mathbb{J}}$ , we have that

$$\sum_{a \in \mathcal{E}_j^{\text{te}}} \varphi_a^s = |\mathbb{B}|. \quad (36)$$

**Proof.** We prove Equality (36) by induction. The equality is satisfied by assumption for  $j = \bar{0}$  (see Equation (3)). Now assume that it is true for  $j \in \hat{\mathbb{J}}$ . We have

$$\sum_{a \in \mathcal{E}_{j+}^{\text{te}}} \varphi_a^s = \sum_{a \in \mathcal{E}_j^{\text{te}}} \varphi_{\theta_j(a)}^s = \sum_{a \in \mathcal{E}_j^{\text{te}}} \varphi_a^s = |\mathbb{B}|,$$

where the first equality is obtained as  $\theta_j$  is bijective, the second one as  $\varphi_a^s = \varphi_{\theta_j(a)}^s$  and the last one by the induction assumption.  $\square$

**Definition 8** A transport planning  $T$  is an arc path in the time-expanded graph  $\mathcal{G}^{\text{te}}$ , that is a sequence of arcs  $T = (a_j)_{j \in \{\bar{0}, \dots, \bar{J}\}}$  satisfying

$$h(a_j) = t(a_{j+}), \quad \forall j \in \{\bar{0}, \dots, \bar{J}\} \quad (37a)$$

$$d(a_j) = j \text{ and } \varphi_{a_j}^s = 1, \quad \forall j \in \hat{\mathbb{J}}. \quad (37b)$$

For an arc  $a$ ,  $t(a)$  denotes its tail node,  $h(a)$  its head node and  $d(a)$  the time index of its tail node, as introduced in Definition 1.

The cardinality of the set  $\{a \in \mathcal{E}_{\bar{0}}^{\text{te}} \mid \varphi_a^s = 1\}$  being  $|\mathbb{B}|$  using Equation (3), we denote its distinct elements as  $\{a_{\bar{0},1}, \dots, a_{\bar{0},|\mathbb{B}|}\}$ . Now, we build  $|\mathbb{B}|$  transport planning as described by the following Proposition 9.

**Proposition 9** For  $b \in \{1, \dots, |\mathbb{B}|\}$ , we consider the arc path  $T^b = (a_j^b)_{j \in \{\bar{0}, \dots, \bar{J}\}}$ , defined recursively by  $a_{\bar{0}}^b = a_{\bar{0}, b}$  and for all  $j$  in  $(\underline{\mathbb{J}} \cup \bar{\mathbb{J}})$  by

$$a_j^b = \theta_j(a_{j^-}^b),$$

where  $\theta_j$  is defined by (34) when  $j \in \underline{\mathbb{J}}$  and by (35) when  $j \in \bar{\mathbb{J}}$ . We have the following properties.

$B_1$  For all  $b \in \{1, \dots, |\mathbb{B}|\}$ , the arc path  $T^b$  is a transportation planning as defined in Definition 8;

$B_2$  For two distinct values  $b, b' \in \mathbb{B}$ , the paths  $T^b$  and  $T^{b'}$  do not have any arc in common;

$B_3$  For each active arc  $a \in \mathcal{E}^{\text{te}}$  such that  $\varphi_a^s = 1$ , there exists a unique storage  $b \in \mathbb{B}$  such that  $a \in T^b$ .

**Proof.** ( $B_1$ ) Fix  $b \in \mathbb{B}$ . We have to check that Equation (37) is satisfied for  $T^b$ . This follows from Lemmas 5 and 6 together with the fact that at initial time  $\varphi_{a_{\bar{0}, b}}^s = 1$  and the flows are preserved by the mapping  $\theta_j$ .

( $B_2$ ) Fix two distinct values  $b, b' \in \mathbb{B}$ . The transport plans  $T^b$  and  $T^{b'}$  differ at the initial time  $\bar{0}$  by construction and then differ at all times as all the mappings  $\theta_j$  for  $j \in (\underline{\mathbb{J}} \cup \bar{\mathbb{J}})$  are injective.

( $B_3$ ) Fix an arc  $a \in \mathcal{E}^{\text{te}}$  such that  $\varphi_a^s = 1$  and consider  $j = d(a)$ . Using ( $B_1$ ), we obtain that the arcs at time  $j$  belonging to the  $|\mathbb{B}|$  transport plans  $\{T^b\}_{b \in \mathbb{B}}$  have a storage flow equal to one and, using ( $B_2$ ), we obtain that they are all distinct. Now, by Lemma 7, the cardinality of set of arcs at time  $j$  with a storage flow equal to one is also  $|\mathbb{B}|$ . Thus, as  $\varphi_a^s = 1$ , there exists a unique storage  $b \in \mathbb{B}$  such that  $a \in T^b$ , which ends the proof.  $\square$

To conclude, we have shown how to construct  $|\mathbb{B}|$  distinct transport plans

$\{T^b\}_{b \in \mathbb{B}}$  that include all active storage flows in  $\varphi^s$ , where  $\varphi^s$  is a feasible storage flow of Problem (27). Algorithm 3 gives the pseudocode to determine  $T^b$  for a given storage  $b \in \mathbb{B}$ . The physical transport planning for a storage  $b$  can be obtained by taking the head of each arc in  $T^b$ .

## 9 Conclusion

In this paper, we tackle an hydrogen transportation problem—in which mobile storages are dynamically routed and swapped—that we called PRP-MI. Modeling the problem using storage (binary) and hydrogen (continuous) flows on a time-expanded graph, we obtain a MILP formulation that captures both the daily scheduling of the mobile storages and the management of inventories. The MA method (direct use of a MILP solver) successfully handles small to medium problem instances within reasonable computational times, and outperforms the greedy heuristic, which is inspired by the heuristic employed by the industrial partner. For larger instances, we introduced the RH method, that first determines a transport planning of the mobile storages, and then, finds the quantity of hydrogen to purchase at the sources and how to allocate it to fill the storages. Numerical experiments indicate that this approach achieves two main results: it provides better results compared to MA for large instance, and it obtains tight lower bounds, while remaining computationally tractable, demonstrating its practical suitability for hydrogen logistics. Future research should integrate stochasticity, as for example in hydrogen demand and in mobile storage transportation times, using similar techniques as the ones used in [20].

---

**Algorithm 3** From flow to storage transport planning
 

---

**Input:** Initial position of the storage  $a_0^b$

```

1:  $T^b \leftarrow (a_0^b)$ 
2: if  $h(a_0^b) \in \mathbb{D}$  then
   at_destination  $\leftarrow$  true
3: else ▷  $h(a_0^b) \in \mathbb{S}$ 
   at_destination  $\leftarrow$  false
4: end if
5: for  $j = 1, \dots, J$  do
6:   if at_destination then
7:      $d \leftarrow h(a_{j-}^b)$ 
8:     Append arc  $(d, d, \underline{j})$  to  $T^b$ 
9:     if  $\sum_{s \in \mathbb{S}} \varphi_{s,d,\underline{j}}^s = 0$  then ▷ No swap occurs at destination  $d$ 
10:      Append arc  $(d, d, \bar{j})$  to  $T^b$  ▷ The storage stays at destination  $d$ 
11:    else ▷ A swap occurs at destination  $d$ 
12:      Find (the unique) source  $s'$  such that  $\varphi_{d,s',\underline{j}}^s = 1$ 
13:      Append arc  $(d, s', \bar{j})$  to  $T^b$  ▷ The storage is sent to source  $s'$ 
14:      at_destination  $\leftarrow$  false
15:    end if
16:  else ▷ at_destination=false
17:     $s \leftarrow h(a_{j-}^b)$ 
18:    Get next arc  $(s, p, \underline{j})$  using  $\sigma_{s,\underline{j}}$  ▷ see Equation (34)
19:    Append arc  $(s, p, \underline{j})$  to  $T^b$ 
20:    if  $p \in \mathbb{D}$  then ▷ The storage is sent to destination  $d$ 
21:      Append arc  $(p, p, \bar{j})$  to  $T^b$ 
22:      at_destination  $\leftarrow$  true
23:    else ▷ The storage stays at source  $s$ 
24:      Append arc  $(s, p, \bar{j})$  to  $T^b$ 
25:    end if
26:  end if
27: end for
28: return  $T^b$ 

```

---

## References

- [1] Y. Adulyasak, J.-F. Cordeau, and R. Jans. Formulations and branch-and-cut algorithms for multivehicle production and inventory routing problems. *INFORMS Journal on Computing*, 26(1):103–120, 2013.
- [2] Y. Adulyasak, J.-F. Cordeau, and R. Jans. The production routing problem: A review of formulations and solution algorithms. *Computers & Operations Research*, 55:141–152, 2015.
- [3] H. Andersson, M. Christiansen, and G. Desaulniers. A new decomposition algorithm for a liquefied natural gas inventory routing problem. *International Journal of Production Research*, 54:1–15, 05 2015.
- [4] C. Archetti, N. Bianchessi, S. Irnich, and M. G. Speranza. Formulations for an inventory routing problem. *International Transactions in Operational Research*, 21(3):353–374, 2014.
- [5] C. Archetti, M. Christiansen, and M. Grazia Speranza. Inventory routing with pickups and deliveries. *European Journal of Operational Research*, 268(1):314–324, 2018.
- [6] M. Avci and S. Topaloglu Yildiz. A mathematical programming-based heuristic for the production routing problem with transshipments. *Computers & Operations Research*, 123:105042, 2020.
- [7] B. M. Baker and M. Ayechev. A genetic algorithm for the vehicle routing problem. *Computers & Operations Research*, 30(5):787–800, 2003.
- [8] T. Benoist, F. Gardi, A. Jeanjean, and B. Estellon. Randomized local search for real-life inventory routing. *Transportation Science*, 45, 08 2011.
- [9] K. Bouanane and Y. Benadada. The multi-plant production routing problem with simultaneous delivery and pickup and recycling, under carbon cap & trade. In *2022 IEEE 6th International Conference on Logistics Operations Management (GOL)*, pages 1–8, 2022.
- [10] L. C. Coelho, J.-F. Cordeau, and G. Laporte. The inventory-routing problem with transshipment. *Computers & Operations Research*, 39(11):2537–2548, 2012.
- [11] L. C. Coelho, J.-F. Cordeau, and G. Laporte. Thirty years of inventory routing. *Transportation Science*, 48(1):1–19, 2014.
- [12] L. Fleischer and E. Tardos. Efficient continuous-time dynamic network flow algorithms. *Operations Research Letters*, 23(3):71–80, 1998.
- [13] C. Füllner and S. Rebennack. Non-convex nested Benders decomposition. *Math. Program.*, 196(1-2):987–1024, 2022.
- [14] Gurobi Optimization, LLC. Gurobi Optimizer Reference Manual, 2023.
- [15] U. Hasturk, A. H. Schrottenboer, E. Ursavas, and K. J. Roodbergen. Stochastic cyclic inventory routing with supply uncertainty: A case in green-hydrogen logistics. *Transportation Science*, 58(2):315–339, Mar. 2024.

- [16] E. Köhler, K. Langkau, and M. Skutella. Time-expanded graphs for flow-dependent transit times. In R. Möhring and R. Raman, editors, *Algorithms — ESA 2002*, pages 599–611, Berlin, Heidelberg, 2002. Springer Berlin Heidelberg.
- [17] J. Lenstra and A. Kan. Complexity of vehicle routing and scheduling problems. *Networks*, 11:221 – 227, 10 2006.
- [18] M. Lubin, O. Dowson, J. Dias Garcia, J. Huchette, B. Legat, and J. P. Vielma. JuMP 1.0: Recent improvements to a modeling language for mathematical optimization. *Mathematical Programming Computation*, 2023.
- [19] F. Margot. *Symmetry in Integer Linear Programming*, pages 647–686. Springer Berlin Heidelberg, Berlin, Heidelberg, 2010.
- [20] A. Parmentier. Learning to approximate industrial problems by operations research classic problems. *Operations Research*, 70(1):606–623, 2022.
- [21] H. R. Peivastehgar, A. Divsalar, M. M. Paydar, and M. Chitsaz. A green production routing problem for medical nitrous oxide: Model and solution approach. *Expert Systems with Applications*, 230:120704, 2023.
- [22] J. Qian and R. Eglese. Fuel emissions optimization in vehicle routing problems with time-varying speeds. *European Journal of Operational Research*, 248(3):840–848, 2016.
- [23] G. M. Sehr, M. Vorbröcker, T. Birth, M. Scheffler, and S. Schiffner. Automated route planning of hydrogen deliveries. In *2022 IEEE 21st Mediterranean Electrotechnical Conference (MELECON)*, pages 1030–1033, 2022.
- [24] C. Shao, C. Feng, M. Shahidehpour, Q. Zhou, X. Wang, and X. Wang. Optimal stochastic operation of integrated electric power and renewable energy with vehicle-based hydrogen energy system. *IEEE Transactions on Power Systems*, 36(5):4310–4321, 2021.
- [25] F. You, J. Pinto, E. García, I. Grossmann, N. Arora, and L. Megan. Optimal distribution-inventory planning of industrial gases. i. fast computational strategies for large-scale problems. *Industrial & Engineering Chemistry Research*, 50, 12 2010.

## A Linearization of constraints

In this Appendix, we prove Lemma 2, by giving a linear reformulation of Constraints (4), (8), (11), (12), (13), (16), (23), and (24) by using additional variables and constraints.

• First, we consider the implications constraints (4) and (13) and (24) and just show how to linearize Constraint (4) as the same mechanism applies to Constraint (13) and (24). The implication constraint

$$\varphi_a^h > 0 \implies \varphi_a^s = 1, \quad \forall a \in \mathcal{E}^{\text{te}}.$$

is equivalent to the following linear constraint

$$\varphi_a^h \leq \bar{S} \varphi_a^s, \quad \forall a \in \mathcal{E}^{\text{te}},$$

where  $\bar{S}$  is the hydrogen flow upper bound (defined in  $A_2$ ). Indeed, if  $\varphi_a^h > 0$ , this inequality forces  $\varphi_a^s = 1$ , because otherwise the

right-hand side would be zero, contradicting the inequality. Conversely, if  $\varphi_a^h = 0$ , the variable  $\varphi_a^s$  is not constrained and can take any value in  $\{0, 1\}$ .

- Second, we address the linearization of the product between a binary variable and a continuous variable present in the right hand side of both Constraints (11) and (12). To linearize the product, we introduce a new variable denoted by  $p$  together with an equality constraint

$$p = \overbrace{\mathbf{1}_{\{0\}} \left( \sum_{s \in \mathbb{S}} \varphi_{s,d,j}^s \right)}^b \varphi_{d,d,j}^h, \quad (38)$$

which remains to be linearized. Noting that the continuous variable  $\varphi_{d,d,j}^h$  is bounded as it belongs to  $[0, \bar{S}]$ , the added nonlinear equality constraint (38) is equivalent to the following set of linear inequalities.

$$p \leq \varphi_{d,d,j}^h, \quad (39a)$$

$$p \leq \bar{S}b, \quad (39b)$$

$$0 \leq p, \quad (39c)$$

$$\varphi_{d,d,j}^h - \bar{S}(1-b) \leq p. \quad (39d)$$

Indeed, we consider two cases. If  $b = 0$ , Constraint (39b) becomes  $p \leq 0$ , which combined with Constraint (39c), implies that  $p = 0$ . Then, Constraint (39d) reduces to  $\varphi_{d,d,j}^h \leq \bar{S}$  and is satisfied. Otherwise, if  $b = 1$ , Constraint (39d) simplifies to  $\varphi_{d,d,j}^h \leq p$  which combined with Constraint (39a), gives  $p = \varphi_{d,d,j}^h$ . Then, Constraint (39b) boils down to  $\varphi_{d,d,j}^h \leq \bar{S}$  which is satisfied. We conclude that Constraints (39) and (38) are equivalent as they share the same solutions for their common variables.

- Third, we move to Constraints (8) and (16) and just show how to linearize Constraint (8) as the same mechanism applies to

Constraint (16). For  $j \in \mathbb{J}$  and  $d \in \mathbb{D}$ , the Constraint (8) reads as follows

$$z_{d,j} = \min(\varphi_{d,d,j}^h, D_{d,j}). \quad (40)$$

By adding a binary variable  $b$  and noting that the continuous variables  $\varphi_{d,d,j}^h$  and  $D_{d,j}$  both belong to  $[0, \bar{S}]$  (using Assumption  $A_2$  for  $D_{d,j}$ ), we show that Constraint (40) is equivalent to the following set of linear constraints (41)

$$z_{d,j} \leq \varphi_{d,d,j}^h, \quad (41a)$$

$$z_{d,j} \leq D_{d,j}, \quad (41b)$$

$$z_{d,j} \geq \varphi_{d,d,j}^h - b\bar{S}, \quad (41c)$$

$$z_{d,j} \geq D_{d,j} - (1-b)\bar{S}. \quad (41d)$$

First, assume that Constraint (40) is satisfied. Then, we have two possible cases or (i)  $z_{d,j} = D_{d,j} \leq \varphi_{d,d,j}^h$  or (ii)  $z_{d,j} = \varphi_{d,d,j}^h \leq D_{d,j}$ . Choosing  $b = 1$  in case (i) and  $b = 0$  in case (ii) straightforwardly give a solution to Constraints (41). Second, the solutions of Constraint (41) are the following. When  $b = 0$ , Constraint (41d) is always satisfied and from Constraints (41a), (41b) and (41c) we obtain that  $z_{d,j} = D_{d,j} \leq \varphi_{d,d,j}^h$ . When  $b = 1$ , Constraint (41c) is always satisfied and from Constraints (41a), (41b) and (41d) we obtain that  $z_{d,j} = \varphi_{d,d,j}^h \leq D_{d,j}$ . Thus, in both cases we obtain that Constraint (40) is satisfied.

- Finally, we fix  $j \in \mathbb{J}$  and  $s \in \mathbb{S}$  and address the linearization of the nondecreasing stock constraint (23) which is satisfied if there exists a bijection  $\sigma_{s,j} : A_{s,j} \rightarrow B_{s,j}$  such that

$$f_{s,l,j}^{\text{in}} \leq f_{s,\sigma_{s,j}(l),j}^{\text{out}}, \quad \forall l \in A_{s,j}. \quad (42)$$

We introduce a matrix  $(\beta_{n,m})_{n,m \in N_s}$  of binary variables, where  $N_s$  is defined in Equation (21), and we prove that Constraint (42)

is equivalent to the set of constraints (43) defined by

$$\sum_{m \in N_s} \beta_{n,m} = y_{s,n,\underline{j}}^{\text{in}}, \quad \forall n \in N_s, \quad (43a)$$

$$\sum_{n \in N_s} \beta_{n,m} = y_{s,m,\underline{j}}^{\text{out}}, \quad \forall m \in N_s, \quad (43b)$$

$$f_{s,n,\underline{j}}^{\text{in}} \leq f_{s,m,\underline{j}}^{\text{out}} + (1 - \beta_{n,m})\bar{S}, \quad \forall n, m \in N_s. \quad (43c)$$

We start by proving that when Constraint (43) is satisfied, there exists a solution to Constraint (42). For that purpose, consider a matrix  $\beta$  and four vectors  $f^{\text{in}}$ ,  $f^{\text{out}}$ ,  $y^{\text{in}}$  and  $y^{\text{out}}$  satisfying Constraints (43). For all  $n \notin A_{s,\underline{j}}$  we have by definition of  $A_{s,\underline{j}}$  that  $y_{s,n,\underline{j}}^{\text{in}} = 0$  and therefore using Constraint (43a) that  $\beta_{n,m} = 0$  for all  $m \in N_s$ . In a similar way, for all  $m \notin B_{s,\underline{j}}$  we have  $y_{s,m,\underline{j}}^{\text{out}} = 0$  and therefore using Constraint (43b) that  $\beta_{n,m} = 0$  for all  $n \in N_s$ . We therefore obtain that, for all  $n \in A_{s,\underline{j}}$ ,

$$\sum_{m \in B_{s,\underline{j}}} \beta_{n,m} + \underbrace{\sum_{m \notin B_{s,\underline{j}}} \beta_{n,m}}_{=0} = y_{s,n,\underline{j}}^{\text{in}} = 1,$$

and, for all  $m \in B_{s,\underline{j}}$ ,

$$\sum_{n \in A_{s,\underline{j}}} \beta_{n,m} + \underbrace{\sum_{n \notin A_{s,\underline{j}}} \beta_{n,m}}_{=0} = y_{s,m,\underline{j}}^{\text{out}} = 1.$$

Thus, the matrix  $\beta$  restricted to  $A_{s,\underline{j}} \times B_{s,\underline{j}}$  is a permutation matrix as a square binary matrix that has exactly one entry of 1 in each

row and each column with all other entries 0. All the elements of the matrix  $\beta$  outside its restriction to  $A_{s,\underline{j}} \times B_{s,\underline{j}}$  have value zero. Now, we build a bijection  $\sigma_{s,\underline{j}} : A_{s,\underline{j}} \rightarrow B_{s,\underline{j}}$  as follows

$$\forall n \in A_{s,\underline{j}}, \quad \{\sigma_{s,\underline{j}}(n)\} = \arg \max_{m \in B_{s,\underline{j}}} \beta_{n,m}. \quad (44)$$

We consider Constraint (43c). First, when  $\beta_{n,m} = 0$ , this constraint reduces to

$$f_{s,n,\underline{j}}^{\text{in}} \leq f_{s,m,\underline{j}}^{\text{out}} + \bar{S}, \quad \forall m \in N_s. \quad (45)$$

which is satisfied as both  $f_{s,n,\underline{j}}^{\text{in}}$  and  $f_{s,m,\underline{j}}^{\text{out}}$  are in  $[0, \bar{S}]$ . Second, when considering the subsets of indices for which  $\beta_{n,m} = 1$ , Constraint (43c) boils down to

$$f_{s,n,\underline{j}}^{\text{in}} \leq f_{s,\sigma_{s,\underline{j}}(n),\underline{j}}^{\text{out}}, \quad \forall n \in A_{s,\underline{j}}, \quad (46)$$

which is precisely Constraint (42).

We prove the converse, that is when Constraint (42) is satisfied, there exists a matrix  $\beta$  satisfying Constraint (43). We consider a bijection  $\sigma_{s,\underline{j}} : A_{s,\underline{j}} \rightarrow B_{s,\underline{j}}$  satisfying Constraint (42) and build a matrix  $\beta$  as follows

$$\beta_{n,m} = \begin{cases} \mathbf{1}_{\{m\}}(\sigma_{s,\underline{j}}(n)) & : n \in A_{s,\underline{j}}, \\ 0 & : n \notin A_{s,\underline{j}}. \end{cases} \quad (47)$$

Using the definition of  $\beta$  and the fact that  $\sigma_{s,\underline{j}}$  is a bijection it is straightforward to obtain that  $\beta$ ,  $f^{\text{in}}$  and  $f^{\text{out}}$  satisfy Constraint (43).